Earth-Abundant 3d Transition Metal Catalysts for Hydroalkoxylation and Hydroamination of Unactivated Alkenes

Lou Rocard [1,2], Donghuang Chen [1], Adrien Stadler [1], Hailong Zhang [1], Richard Gil [1], Sophie Bezzenine [1] and Jerome Hannedouche [1,*]

[1] Institut de Chimie Moléculaire et des Matériaux d'Orsay (ICMMO), Université Paris-Saclay, CNRS, CEDEX, 91405 Orsay, France; lou.rocard@ens-cachan.fr (L.R.); donghuang.chen@universite-paris-saclay.fr (D.C.); adrien.stadler@universite-paris-saclay.fr (A.S.); hailong.zhang@universite-paris-saclay.fr (H.Z.); richard.gil@universite-paris-saclay.fr (R.G.); sophie.bezzenine@universite-paris-saclay.fr (S.B.)

[2] Laboratoire de Photophysique et Photochimie Supramoléculaires et Macromoléculaires (PPSM), ENS Paris-Saclay, Université Paris-Saclay, CNRS, 91190 Gif-sur-Yvette, France

* Correspondence: jerome.hannedouche@universite-paris-saclay.fr

Abstract: This review summarizes the most noteworthy achievements in the field of C–O and C–N bond formation by hydroalkoxylation and hydroamination reactions on unactivated alkenes (including 1,2- and 1,3-dienes) promoted by earth-abundant 3d transition metal catalysts based on manganese, iron, cobalt, nickel, copper and zinc. The relevant literature from 2012 until early 2021 has been covered.

Keywords: earth-abundant 3d transition metals; hydroalkoxylation; hydroamination; alkenes; amines; ethers; alcohols

1. Introduction

The prevalence of ether and amine motifs in various areas of chemistry, such as bulk and fine chemicals, biological and pharmaceutical chemistry or catalysis, has driven the development of original and innovative methods for their efficient synthesis [1,2]. Among these methods, the most attractive and atom-economical approach towards these prevalent motifs is undoubtedly the addition of E–H (E = O, N) σ-bond onto unactivated alkenes, referred to as alkene hydrofunctionalization [3–9]. This route is also step-economical and benefits from relatively available and inexpensive starting materials. However, the inherent electronic repulsion between the olefin π-electrons and the nonbonding lone pair of the heteroatom renders this approach kinetically challenging in the absence of a catalyst. Control of the regioselectivity and enantioselectivity of the process to access (enantioenriched) key building blocks are also essential issues that need to be tackled for a broad synthetic use of the methodology. In light of these challenges, a variety of elegant activation strategies has been developed over the years to address some of these issues and extend the methodology potential to access various classes of O- and N-containing compounds. For several decades, the field has been dominated with successes by Group 1–4 elements and noble metals-based catalysts that operate through a two-electron reactivity by either amine activation (via deprotonation) or alkene activation (via metal coordination) [10–16]. The current booming trend for the use of earth-abundant, first-row late transition metal, metal-free and photoredox processes in catalysis has reshaped the field of alkene hydrofunctionalization giving birth to efficient strategies that not only rely on classical activation modes but also on novel radical-type reactivities [9,10,17–19]. For examples, photo-mediated E–H (E = O, N) bond addition on electron-rich alkenes wherein single-electron oxidation of one of the nucleophilic partners furnishes an electrophilic oxygen- [20], nitrogen- [18,21–27] or carbon- [28–32] centered radical cation that can be intercepted by the second nucleophilic partner has become a valuable tool for the construction of C–E (E = O, N) bond by an

anti-Markovnikov hydrofunctionalization process. Designed chiral Brønsted acids with specific confined environments have successfully enabled the contemporary challenge of asymmetric cyclohydroalkoxylation of aliphatic alcohols tethered to 1,1-disubstituted alkenes [33,34].

This review will survey the most relevant achievements in the field of intra- and intermolecular hydroalkoxylation and hydroamination of unactivated alkenes (including 1,2- and 1,3-dienes) promoted by earth-abundant 3d transition metal catalysts from manganese to zinc. It is beyond the scope of this review to cover all the growing activity of alkene hydrofunctionalization and, in this context, the literature coverage has been restricted from 2012 until early 2021 albeit a few related reports that appeared earlier are mentioned. For earlier developments, the readers are invited to refer to previous reviews on the topic [6–8]. Relevant breakthroughs in the direct addition of electronically biased amines (such sulfonamides, amides, etc.) onto unactivated olefins will also be covered but the term hydroamidation will be preferred to refer to these compounds bearing electron-withdrawing substituents. The O–H bond formation reactions by hydration [35,36] or hydroacyloxylation [37–39] of unactivated alkenes are not included in this survey. The achievements are summarized according to the nature of the 3d transition metal and the type of hydrofunctionalization reaction.

2. Manganese

Despite the interesting features of being of low toxicity and eco-friendly, manganese remains unexploited for the development of catalytic hydroamination and hydroalkoxylation methodologies of unactivated alkenes [40]. To our knowledge, there is only one report of manganese-catalyzed hydroamination of unactivated alkenes [41,42]. This year, the group of Qu and Zhang reported an elegant visible-light-induced manganese-promoted N–F bond activation strategy to generate amidyl radicals from *N*-fluorinated sulfonamides (Figure 1). These electrophilic amidyl radicals can react with olefins in the presence of hydrosilane to afford a rich variety of *N*-sulfonamides pyrrolidines and functionalized linear *N*-sulfonamides by *exo*-cyclization and anti-Markovnikov addition respectively. The intermolecular process is restricted to styrene derivatives, 2-vinylthiophene and electron-rich alkenes, such as vinyl sulfides and vinyl ethers. Indeed, due to electronic matching problems, low reactivity is observed for alkyl-substituted alkenes. This protocol can also be applied to a two- and three-component carboamination of alkenes [41]. The authors proposed that a light-induced homolysis of the Mn–Mn bond in $Mn_2(CO)_{10}$ generates a metalloradical $Mn(CO)_5$ having the ability to abstract the F atom from the substrate and leading to the formation of the reactive amidyl radicals [43]. Subsequent regioselective addition of these *N*-centered radicals to the alkenes leads after silane-mediated HAT to the formation of the product. From mechanistic investigations, it is proposed that two competitive radical chain reactions, one of which including metallic species, complete the catalytic cycle.

Qu and Zhang 2021
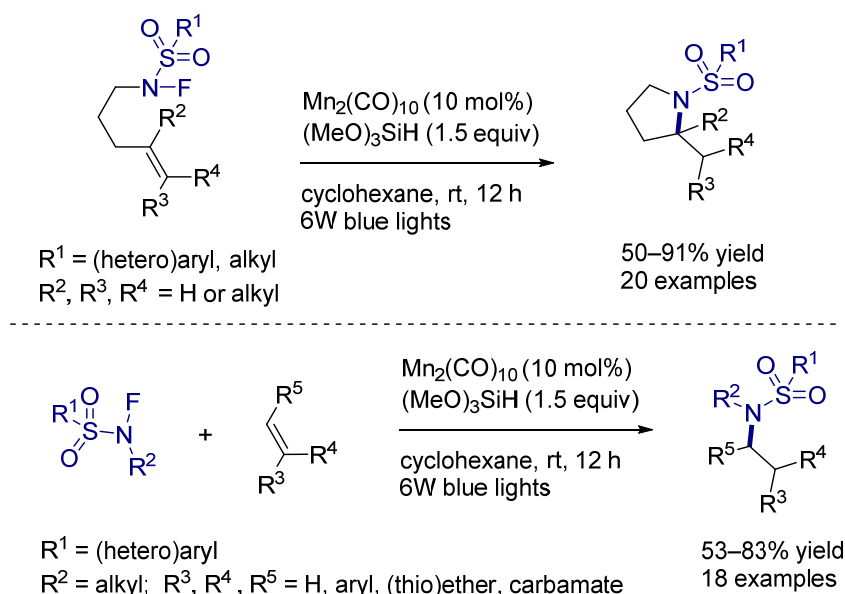
Figure 1. Visible-light induced manganese-catalyzed alkene hydroamination with *N*-fluorinated sulfonamides. rt = room temperature.

3. Iron

3.1. Hydroalkoxylation

In the 2010s, intra- and intermolecular hydroalkoxylation of unactivated alkenes emerged using Lewis acid iron salts as catalysts [44]. Indeed, inexpensive and poorly toxic iron (III) chloride mainly associated with various additives, such as silver triflate or *p*-toluenesulfonic acid, afford effective Lewis acid catalysts for various hydroalkoxylation reactions involving alkene derivatives of various substitution patterns [45,46]. Nevertheless, in 2007, the Takaki group demonstrated that cationic iron complexes generated by the combination of FeCl$_3$ and AgOTf enable the efficient cyclohydroalkoxylation of various alkenes under mild conditions [47]. Several years later, Zhou et al. reported a Markovnikov selectivity intermolecular version involving aliphatic alcohols with styrene derivatives and 1-octene using the FeCl$_3$/TsOH combination [48]. Iron (III) chloride can also be supported on montmorillonite as natural inorganic material to provide a very effective heterogeneous and reusable catalyst for this process. In 2015, the supported Fe-MMT catalyst developed by Antoniotti et al. showed good activity and selectivity at 80 °C in dimethyl carbonate (DMC) for the cyclization of alkenols with various substitution patterns on the alkene moiety (Figure 2) [49,50]. This heterogeneous catalyst, which can be reused several times without loss of activity, displays higher activity and selectivity than those of reactions carried out under homogeneous catalysis. The system was demonstrated to proceed under truly heterogeneous catalysis and can be transferred to an intermolecular process despite lower efficiency.

In 2012, Kang et al. developed an efficient catalytic system for the *exo*-cyclohydroalkoxylation of trialkylated δ-allenyl alcohols observing isomerization or no isomerization of the product alkene moiety depending on the nature of the iron counterion and the operating conditions as illustrated in Figure 3 (top) [51]. This methodology is restricted to trialkylated allenols as mono- and dialkylated did not undergo cyclization under these conditions. The Fe(OTs)$_3$ system can also be applied to the cyclization of γ-allenyl alcohols with concomitant alkene isomerization (Figure 3, top) [52]. During the reactivity study of γ-cyclohexyl-substituted allenic alcohols by this catalytic system, it was shown that the temperature influences not only the isomerization of the hydroalkoxylation products but also the *endo*/*exo*-methylene selectivity.
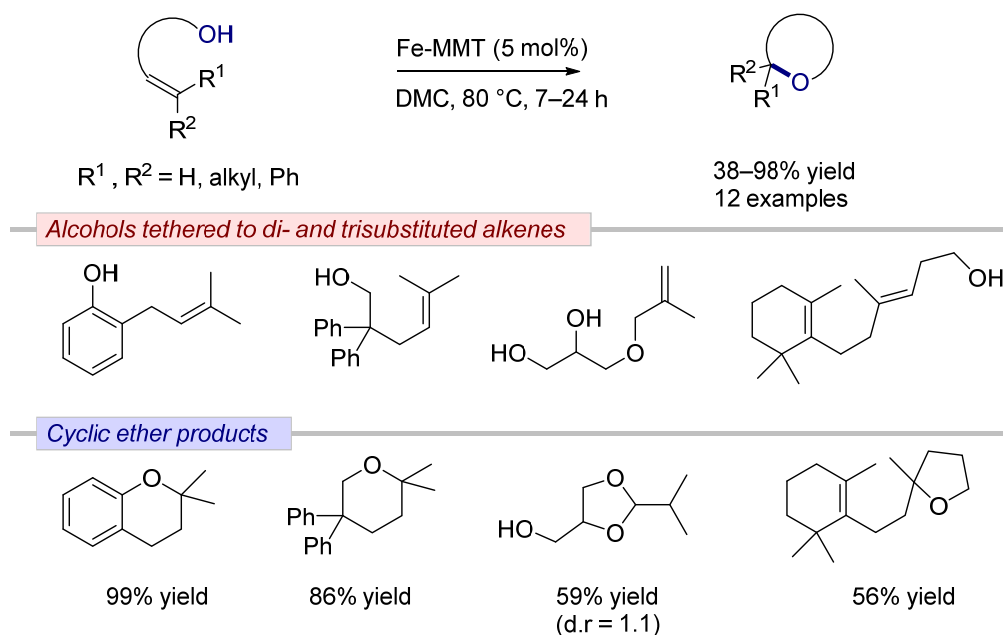
Antoniotti 2015

R^1, R^2 = H, alkyl, Ph

38–98% yield
12 examples

Alcohols tethered to di- and trisubstituted alkenes

Cyclic ether products

99% yield　　86% yield　　59% yield (d.r = 1.1)　　56% yield

Figure 2. Cyclohydroalkoxylation of alkenes catalyzed by Fe-MMT. d.r = diastereomeric ratio.

Kang 2012

R^1 = H, Ph; R^2 = H, CH$_3$
R^1, R^2 = (CH$_2$)$_4$, (CH$_2$)$_5$
R^3 = H, Ph, CH$_3$,CH$_2$CHCH$_2$,CCH
R^4 = H, CH$_2$OH, CH$_2$OBz; n = 0, 1

23–91% yield
9 examples

n = 1
79–96% yield
6 examples

n = 0
34–56% yield
9 examples

R^1, R^2 = (CH$_2$)$_4$, (CH$_2$)$_5$, H, alkyl, Ph

31-83% yield
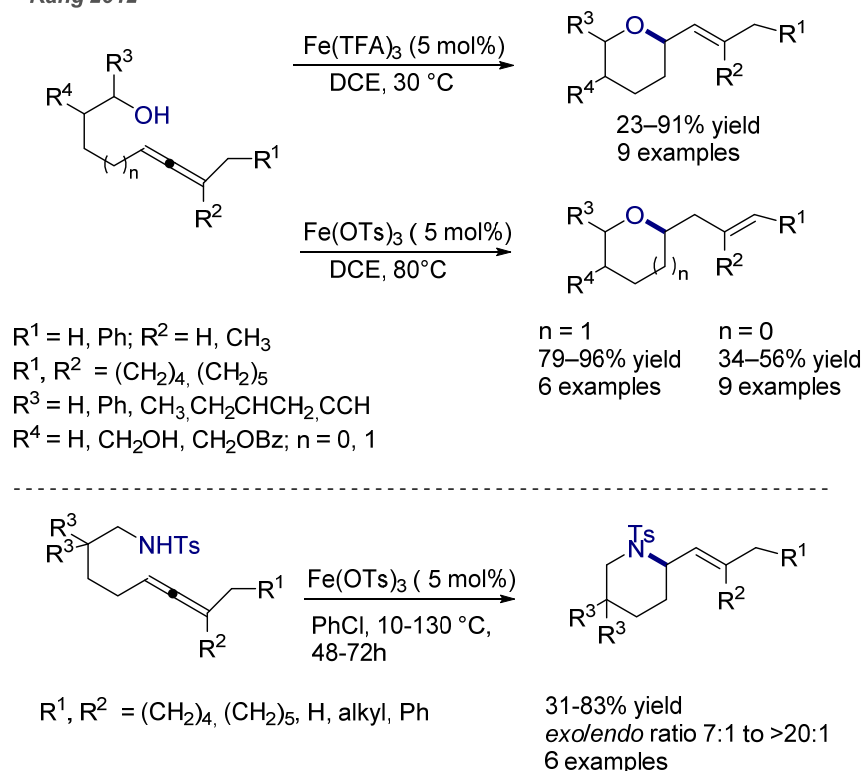*exo/endo* ratio 7:1 to >20:1
6 examples

Figure 3. Syntheses of tetrahydropyrans, furans and *N*-tosyl piperidines from cyclohydrofunctionalization reaction of allenols and allenamides catalyzed by Fe(TFA)$_3$ and Fe(OTs)$_3$.

More recently, Rueping and co-workers have developed and used as a precatalyst the air and moisture stable tetraphenyl-substituted cyclopentadienone iron(0) tricarbonyl complex, easily prepared from tetraphenylcyclopentadienone and iron pentacarbonyl (Figure 4) [53]. This complex was efficient for the *exo*-cyclohydrofunctionalization of α-allenic tethered to secondary alcohols or *N*-Cbz protected amines providing the correspond-

ing 2,3-dihydrofurans or 2,3-dihydropyrroles in good yields and high chemoselectivity. The authors presumed that the first step of the mechanism is the formation of the competent 16-electron iron species by trimethylamine *N*-oxide promoted decarbonylation of tricarbonyl precatalyst **1-Fe**. Subsequent dual activation of the substrate by the metal-ligand bifunctional iron catalyst, through hydrogen-bonding between the C=O of the ligand and the *O*- or *N*-nucleophile and metal coordination of the allene, allows the C-heteroatom bond formation to occur. This step leads to the formation of an iron vinylidene intermediate, which isomerizes into a more stable complex by two consecutive hydrogen transfers implying the cyclopentadienone ligand. Protodemetalation of the more stable vinylidene intermediate leads to the liberation of the desired product. The reaction chemoselectivity in favor of 2,3-dihydrofuran is controlled by the formation of the more stable vinylidene iron complex.
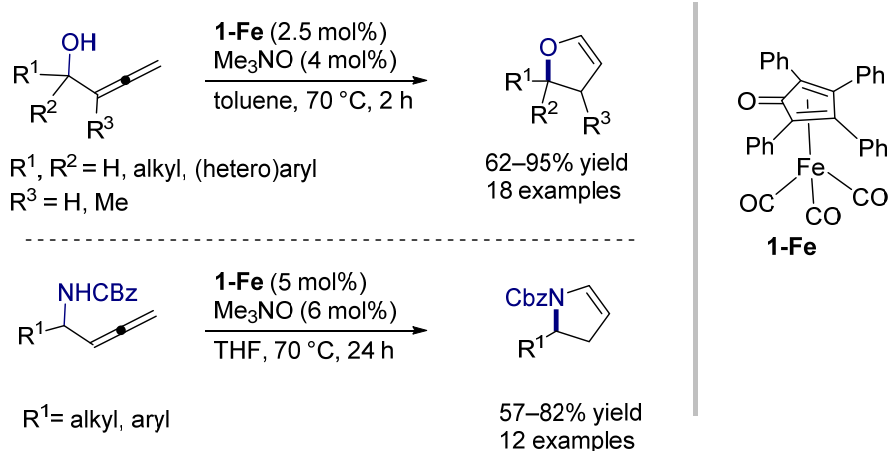
Figure 4. Syntheses of 2,3-dihydrofurans and 2,3-dihydropyrroles by cyclohydrofunctionalization promoted by tetraphenyl-substituted cyclopentadienone iron(0) tricarbonyl precatalyst **1-Fe**.

In 2019, Marcyk and Cook described a very efficient method for intermolecular C–O and C–N bond formation by Markovnikov alkene hydrofunctionalization using a cationic iron(III) system (Figure 5) [54]. From various primary and secondary alcohols and mono-, di- and trisubstituted alkenes, they produced different ethers in moderate-to-good yields under very mild conditions using the air- and moisture-tolerant combination $FeCl_3/AgSbF_6$. In order to avoid deleterious substitution reactions leading to side products, primary alcohols were preferred. Furthermore, it is necessary to employ an excess of alkenes (3 equiv) to override the lower reactivity of alcohols with respect to sulfonamides. The study of the scope of the alcohol partner on cyclohexene indicates that the best results were obtained with alcohols substituted by an electronic deficient aromatic group such as 2-(4-nitrophenyl)-ethanol. This latter was then used with various cyclic and acyclic alkenes (Figure 5). It is worth noting that unsymmetric monoalkene 1-hexene affords a mixture of 2- and 3-substituted hydro-functionalized products likely due to a carbocation rearrangement. Additionally, trisubstituted alkenes gave superior yields with iron trichloride alone due to reduced competitive olefin dimerization.

Cook 2019
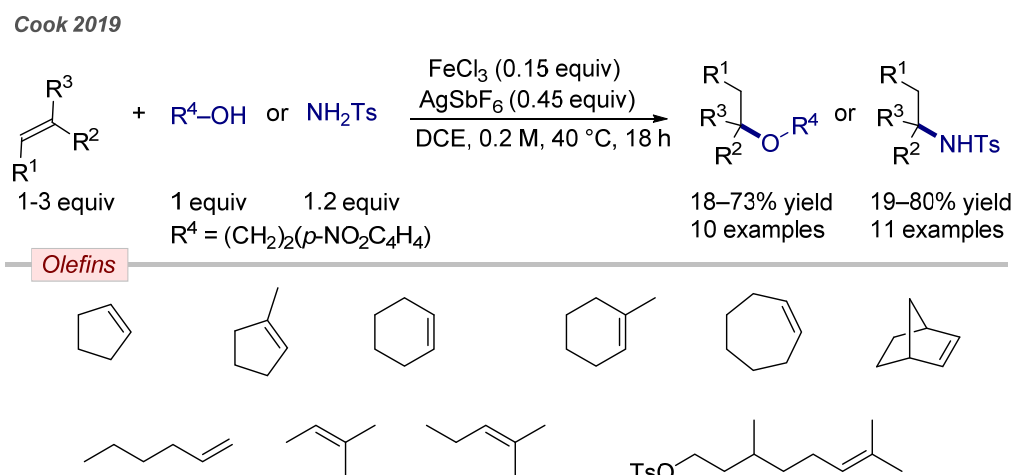
Figure 5. Intermolecular hydrofunctionalization of mono-, di- and trisubstituted olefins with 2-(4-nitrophenyl)-ethanol and *p*-toluenesulfonamide catalyzed by the combination FeCl₃/AgSbF₆.

3.2. Hydroamination

Until 2014, only iron (III) salts were reported in the literature as effective Lewis acid catalysts for intra or intermolecular C–N bond formation by hydroamidation of unactivated alkenes mainly from *N*-tosylamines, but regioselectivity issues were observed in some cases [55–58]. In 2012, the group of Kang extended the Fe(OTs)₃-based protocol developed for the cyclization of δ-allenyl alcohols to the intramolecular hydroamidation of δ-allenyl amines (Figure 3, bottom). In contrast to the hydroalkoxylation reaction, which was restricted to trialkylated substituted allene moiety, this extension was efficient for the cyclization of *N*-tosyl amines tethered to mono-, di- and trisubstituted alkenes [51]. However, the corresponding *N*-tosylpiperidines from trialkylated allenyl amines were obtained as an inseparable mixture of products resulting from double bond isomerization from *exo*-methylene to *endo*-methylene. A similar transformation was later applied by Wang in cascade reactions implying arylamines and propargylic alcohols catalyzed by FeCl₃·6H₂O [59]. In 2016, it was described a highly effective diastereoselective FeCl₃-catalyzed hydroamidation of α-substituted aminoalkenes derived from enantiopure starting materials, such as amino acids, and this methodology was applied to the enantiodivergent synthesis of (+)- and (−)-pyrrolidine 197B [60].

Recently, as for hydroalkoxylation, new developments have been described using iron for the hydroamidation of unactivated alkenes. In 2019, as mentioned above, Marcyk and Cook described the use of a combination of FeCl₃ and AgSbF₆ to functionalize mono-, di-, and trisubstituted olefins with a wide range of sulfonamide nucleophiles proceeding in very mild conditions with Markovnikov selectivity (Figure 5) [54]. No hydroamination product was observed with other electron-deficient protecting groups on the amine due to stronger binding to the cationic metal. This catalytic system was applied to a cascade process for the synthesis of tetrahydroisoquinolines [61]. The tetraphenyl-substituted cyclopentadienone iron(0) tricarbonyl complex was also efficiently used as a precatalyst for the *endo*-cyclohydroamidation of *N*-Cbz protected amines tethered to monoallenes (Figure 4, bottom) [53]. The unusual selectivity leading to cyclic enamines was explained by dual activation of the substrate by the iron-based metal−ligand catalyst.

Recently, C–N bond formation by hydroamination of unactivated alkenes with unbiased amines has also been described with iron(III) salts as Lewis acid catalysts. An interesting anti-Markovnikov hydroamination of vinylpyridines with azoles including diazoles and triazoles, catalyzed by FeCl₃ was recently reported (Figure 6, top) [62]. The reaction proceeded at 110 °C and gave moderate-to-excellent yields. The authors explained the unusual anti-Markovnikov selectivity by FeCl₃ activation of the *N*-atom of the vinylpyridine to form a zwitterionic intermediate, which is in equilibrium with one
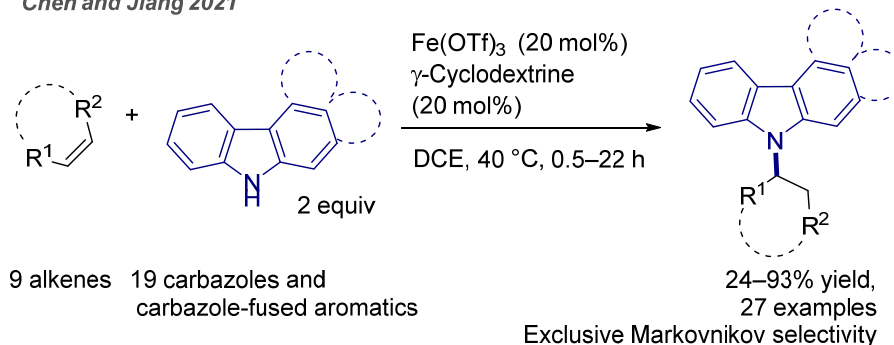
containing a positive charge on the terminal carbon of the vinyl group and subsequent conjugate addition of the azole.
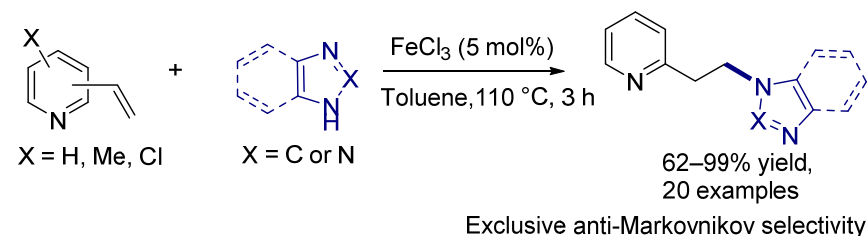

Figure 6. Selective intermolecular iron(III)-catalyzed alkene hydroamination with *N*-heterocycles.

Last year, Chen, Jiang and co-workers published a general catalytic system, composed of Fe(OTf)$_3$ and γ-cyclodextrin, for the Markovnikov selective hydroamination of styrenes (and norbornene) with carbazoles and carbazole-fused aromatics with high activity and selectivity under mild conditions (Figure 6, bottom) [63]. The scope of the alkenes and the carbazoles has been studied. The authors have shown that monosubstituted styrenes bearing electron-donating or electron-withdrawing groups, but also a bulky functional are well tolerated. Limitations appear with the use of larger alkenes than monosubstituted styrene such as 2-vinylnaphtalene. Concerning the use of aliphatic alkenes, norbornene also furnishes the hydroamination product under the standard conditions contrary to cyclohexene which remains inert. No limit in size of the carbazoles was observed, as various carbazole-fused aromatics provide the hydroamination products moderate-to-good yields. The authors proposed that bulky Fe(OTf)$_3$ coordinates at the narrower rim of cyclodextrins through hydrogen bonds with the primary hydroxyl groups to form in situ a highly active Fe(OTf)$_3$/cyclodextrine complex. The complex thus formed would then deprotonate the carbazole to generate the active iron species that would react with the styrene derivatives captured in the cyclodextrin cavity.

The first example of regioselective hydroamination of electronically unbiased amines catalyzed by iron complexes was described by the Hannedouche group in 2014 (Figure 7) [64]. In this work, the use of structurally defined C_2-symmetric low-coordinate β-diketiminatoiron(II)-alkyl complex **2a-Fe** in the presence of cyclopentylamine as co-catalyst allows the formation of pyrrolidines and piperidines in good-to-excellent yields at 90 °C. This catalytic system requires aminoalkenes with a geminal disubstitution on the tether and does not proceed with 1,2-dialkylsubstituted alkenes. Mechanistic studies have shown that the activation pathway proceeds by initial deprotonation of the amine and involves a migratory 1,2-insertion of the alkene in an iron-amido bond of an isolable amido iron complex followed by a rate determining aminolysis step. It should be noted that the presence of cyclopentylamine, a non cyclizable primary amine as co-catalyst diminishes the formation of β-H elimination products but also reduces the reaction rate. To overcome this limitation and relying on experimental and computational mechanistic studies, the

group subsequently developed the synthesis of a variety of well-defined C_1-symmetric β-diketiminatoiron(II)-alkyl complexes that differ by the nature of one aryl group on the *N*-atom and studied their reactivities [65]. It was shown that steric effects and/or the coordinating ability of an *ortho*-methoxy substituent on one *N*-aryl rings of the β-diketiminate affords a more active and selective catalyst **2b-Fe** than the catalytic system C_2-symmetric **2a-Fe**/cyclopentylamine (Figure 7) [66].

Hannedouche 2014
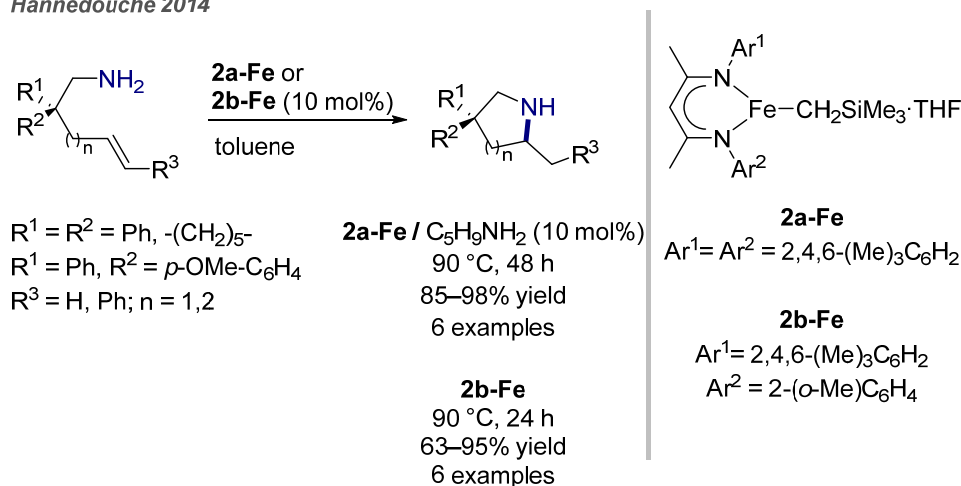
Figure 7. Cyclohydroamination of primary amines tethered to unactivated alkenes catalyzed by well-defined β-diketiminatoiron(II) alkyl complexes.

In 2014, an umpolung electrophilic amination was reported by Yang and co-workers as an alternative strategy to the classical hydroamination, similarly to the copper-hydride strategy reported by Buchwald, Hirano and Miura (vide infra) (Figure 8) [67]. After an optimization study, a combination of $FeCl_2$ and 2,6-diiminopyridine as precatalyst in the presence of four equivalents of cyclopentylmagnesium bromide as reducing agent showed its effectiveness for the regioselective Markovnikov hydroamination of a wide range of aromatic olefins and hydroxylamine esters as the electrophilic nitrogen source. The authors proposed that the catalytic cycle is based on in situ formation of a Fe–H species but unlike to the CuH methodology (vide infra), it is inefficient for the transformation of α- and β-methylstyrenes, *p*-Cl- and *p*-CF_3-styrenes and aliphatic terminal alkenes.

*Yang 2014*
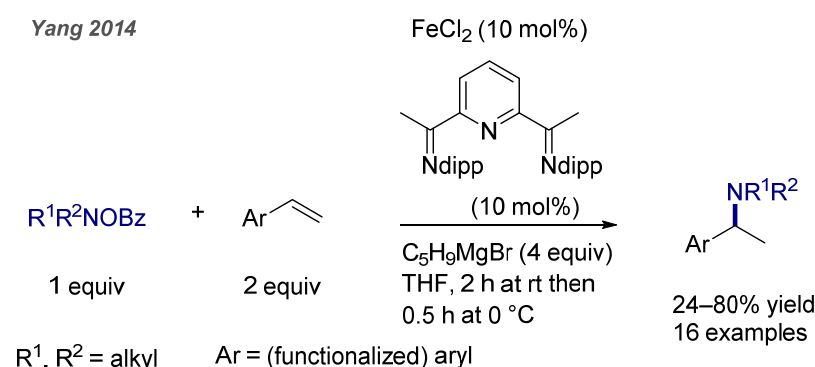
Figure 8. Markovnikov selective iron-catalyzed hydroamination of vinylarenes with hydroxylamine esters. rt = room temperature.

In 2015, the group of Baran described a practical formal hydroamination process based on iron hydride chemistry for the preparation of secondary (hetero) arylamines substituted by secondary or tertiary alkyl groups from nitro (hetero)arenes and mono-

and polysubstituted alkenes (Figure 9, top) [68]. This system stems from their expertise on the H-atom transfer (HAT) promoted by Fe(III)–H for C–C bond radical formations from alkenes [69]. Using iron(III) acetylacetonate (30 mol%) and phenylsilane (2–3 equiv), compatible with air and moisture, a wide variety of hindered (hetero) aryl secondary amines were prepared in low-to-good yields and with full Markovnikov selectivity. In this process, [Fe^n]–H species (generated in situ from iron (III) acetylacetonate and phenylsilane) [70] allows the formal single electron reduction of the nitro (hetero) arene and olefin to a nitroso (hetero) arene and an alkyl radical by regioselective HAT respectively. The formal hydroamination product is then obtained by attacking the alkyl radical on the nitroso (hetero) arene to lead to an O-centered radical species, which are subsequently involved in ethanolysis and SET [71]. A considerable advantage of this system over other C–N bond formation methods is its compatibility with a remarkable number of functional groups. Indeed, this methodology has a wide tolerance for amide, amine, alcohol, thioether, ketone, halide, nitrile, triflate and boronic acid. However, this protocol requires the use of an excess of alkene and is limited to nitro (hetero) arenes (excluding 2-nitropyridines, nitroimidazole and nitrophenyl having orthoesters or thiols or free alcohols) and aliphatic alkenes as substituted styrenes give low yields. A year later, the groups of Shenvi [72] and Thomas and Shaver [73,74] independently optimized the catalytic system developed by Baran by using either isopropoxy (phenyl) silane instead of phenylsilane, or an amine—iron(III) bis (phenolate) complex instead of iron(III) acetylacetonate. The catalyst loading could be reduced, and the reaction carried out at room temperature under these new conditions.
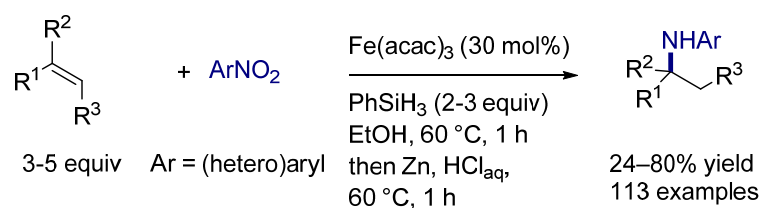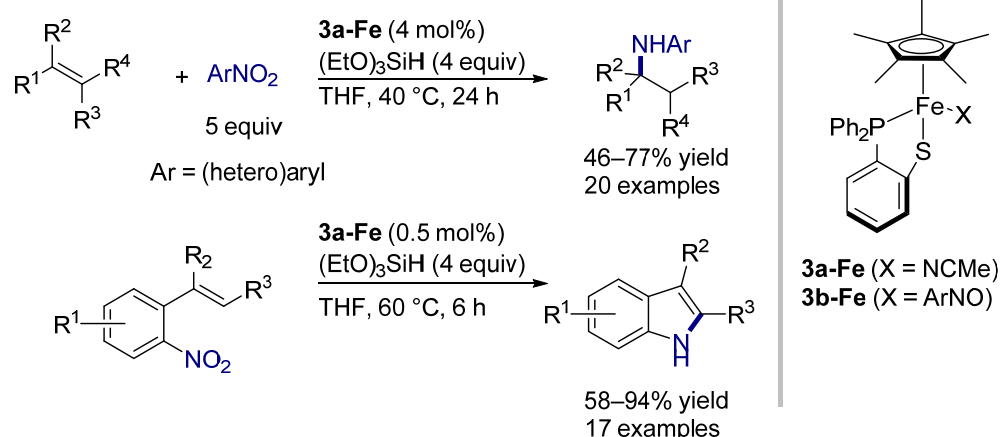
Figure 9. Inter and intramolecular Fe-H-promoted formal hydroamination of nitro (hetero)arenes and alkenes.

Last year, the Wang's group extended the scope of these reductive C–N bond formations using a new system composed from a single half-sandwich iron(II) complex and (EtO)₃SiH for the synthesis of various secondary branched amines and indole derivatives by respectively inter or intramolecular reductive coupling (Figure 9, bottom) [75]. The authors showed that the complex **3a-Fe** reacts with nitro (hetero)arenes to afford iron-nitrosoarene complex **3b-Fe**, which can be isolated and allows the formation of arylamines

from nitroarenes and alkenes in the presence of $(EtO)_3SiH$. In contrast to the Baran system which is low-yielding for arylarenes and required a reductive workup (Zn/HCl_{aq}), this catalytic system affords secondary amines in moderate-to-high yields from both aliphatic and aryl alkenes and in the presence of hydrosilane as the only reducing agent. For the intermolecular C–N bond coupling with styrene derivatives, electron-donating groups at the para position of the phenyl ring give better yields than electron-withdrawing, such as the cyano group, although the latter is compatible with the reaction. Nevertheless, aliphatic alkenes are generally less reactive than aromatic alkenes. As shown in Figure 9, a low catalyst loading (0.5 mol%) is enough to provide the indole products in very good yields. Fused tricyclic indole derivatives, 2,3-disubstituted indoles, 3-phenylindole but also indazole can be formed in good yields and functional group like OMe, F, Br and CF_3 are tolerated by the catalytic system.

4. Cobalt

4.1. Hydroalkoxylation

Cobalt catalysis has been widely studied for the development of hydrofunctionalization reactions of alkenes through the generation of alkyl radicals by metal-hydride hydrogen atom transfer (MHAT), which can subsequently be intercepted by heteroatom-based radicalophiles to create a C-heteroatom bond [76]. Mukaiyama and Isayama originally described the use of $Co(acac)_2$, with silane and molecular oxygen, for the hydration of olefin [77]. This metal was further exploited by Carreira for the introduction of various other functional groups (hydrazine, azide, cyanine, chlorine, oxime) using Co catalysts (such as **4a-Co**, Figure 10) [78–81].

In 2013, with the aim of developing further hydrofunctionalization reaction (i.e., fluorination), Shigehisa, Hiroya and co-workers serendipitously found out that cobalt-Schiff base catalyst **4a-Co** in the presence of *N*-fluorotrimethylpyridinium salts ($Me_3NFPYBF_4$ or $Me_3NFPYOTf$) and a hydrosilane reagent can promote the hydroalkoxylation of unactivated alkenes with alcohol solvents, such as MeOH or *t*-BuOH (Figure 10, top) or fluorinated alcohols [82,83]. The authors demonstrated the versatility of the reaction, able to tolerate a wide range of functionalities (silyl, acetal, esters, amides, nitro, tosylates, heterocycles, etc.) and applicable to mono-, di- and tri-substituted olefins. The postulated mechanism involves the formation of a cobalt(III)-fluoride complex followed by its transformation into Co(III) –H with the silane derivative. Then, the reaction of Co–H and alkene via an MHAT process affords the chemoselective generation of C-centered radical, which is further converted into a cation intermediate by a radical-polar crossover reaction facilitated by the *N*-fluorocollidinium salt and/or the cobalt-Schiff base catalyst. Trapping of the reactive cation by the nucleophilic alcohol gives the expected product (after deprotonation by 2,4,6-trimethylpyridine). A similar system was also used for the redox-switchable hydroalkoxylation of styrenes by incorporating a ferrocene ligand on the Co catalyst, able to modulate its reactivity in an on/off manner [84].

In 2016, Shigehisa and co-workers further exploited their system and reported intramolecular hydroalkoxylation of alkenols (Figure 10, bottom) [85]. Under similar conditions using catalyst **4a-Co**, 5- and 6-membered rings were efficiently formed (70–97% yields) using aliphatic and benzylic alcohols (as well as carboxylic acids). However, phenol cyclization was found to be unsuitable for the reaction (<13% yield). For the synthesis of medium-ring products, such as 7–9-membered cyclic ethers and lactones, catalyst **4b-Co** gave better results. As an example, an oxepane derivative product was obtained in 60% yield (vs. 30% using **4a-Co**). Interestingly, when using protected alcohols bearing TBS (*tert*-butyldimethylsilyl), MOM (methoxy acetal) or Bn (benzyl) groups, deprotective cylizations were carried out directly affording the cyclic ethers. This was of particular interest for carrying efficiently phenolic cyclizations (2 examples: 70–90% yield using MOM groups) circumventing the reactivity issue observed with protecting-group free phenol substrates. More recently, this deprotective cyclization strategy was successfully exploited for the preparation of cyclic carbamates and isourea [86]. The mechanistic investigations revealed

that cyclization should occur by simultaneous radical oxidation and nucleophilic trapping in a concerted transition state, leading to the formation of an oxonium intermediate followed by deprotection. In addition, the authors noted that incorporating chiral elements within the catalyst can lead to the observation of an enantioselectivity, which suggests that the cobalt should interfere within the C–O bond-forming transition state involving a cationic Co complex [84].
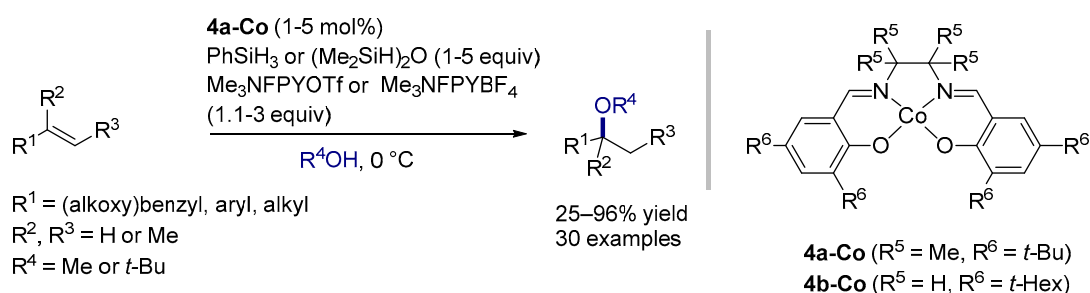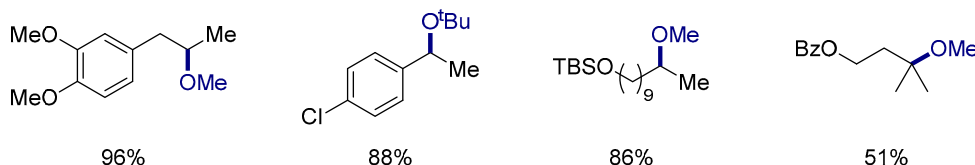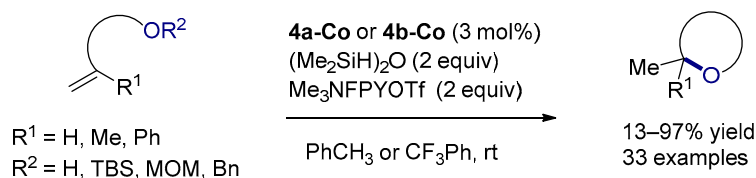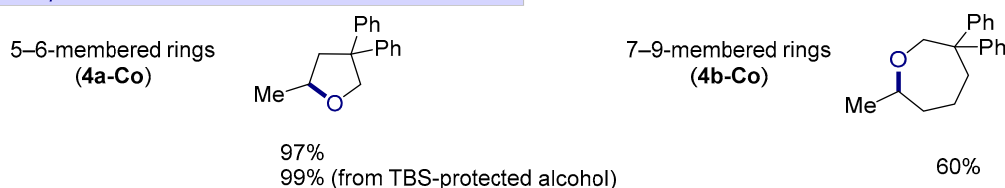

Figure 10. Co-salen promoted hydroalkoxylation of unactivated alkenes. rt = room temperature.

In 2018, using a similar Co–H mediated HAT/radical-polar crossover strategy, the group of Pronin reported a Co-Schiff base-catalyzed hydrofunctionalization of tertiary allylic alcohols that, under ligand control, selectively produces either the corresponding epoxides or semipinacol rearrangements products (Figure 11) [87]. Cyclohexanol (but not cycloheptanol or cyclopentanol) derivatives and 2-methylbut-3-en-2-ol form the corresponding epoxides in yields up to 69% when Co-salen **4c-Co** is employed under the reactions conditions described in Figure 11 (top). Interestingly, switching the 1,2-diphenylethylenediamine backbone of the salen ligand by 2,3-dimethylbutane-2,3-diamine or replacing the *p-tert*-butyl substituents of the catalyst by nitro groups leads to a change in reaction outcome and allows the efficient formation of the corresponding ketone products from semipinacol rearrangement. This strong ligand-dependence of the hydrofunctionalization outcome and additional experiments suggest that the epoxidation reaction involves alkylcobalt(IV) complexes as electrophilic intermediates. Recently, the same research group

has explored further the effect of the ligand structure on the enantioenrichment of the epoxidation reaction [88]. Extensive variation of the 1,2-diphenylethylenediamine fragment of the ligand led to the identification of dibenzofuran-containing Co-catalyst **4d-Co** as the optimal catalyst affording 4-vinyltetrahydro-2H-pyran-4-ol in 69% yield and with 95% enantiomeric excess (ee) (Figure 11). In contrast, **4c-Co** afforded the corresponding epoxide in 60% yield and with 15% ee. Good performance was also observed for various vinyl-carbinols derivatives from 4-disubstituted cyclohexane, tetrahydropyran or piperidines (Figure 11). However, when applied to acyclic structures, no enrichment was obtained, while 5- or 7-membered ring-containing substrates did not afford the corresponding epoxides but led to the semipinacol rearrangement products. Mechanistically, the authors proposed the presence of cationic alkylcolbalt(IV) complexes in the enantio-determining step, where cation-π interactions between the radical cation of the Schiff base fragment and the biaryl substituents of the dibenzofuran motif, account for the superior asymmetric induction observed with **4d-Co** [87].
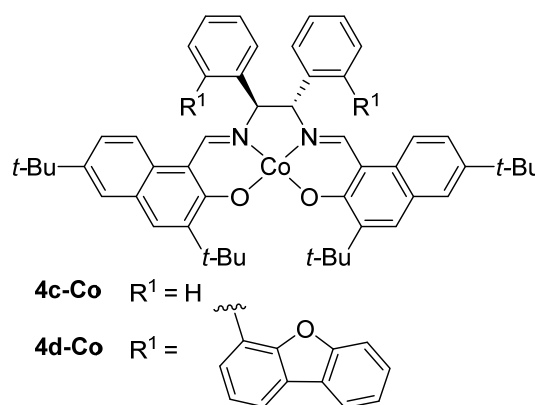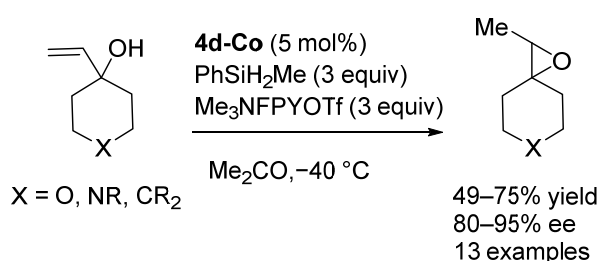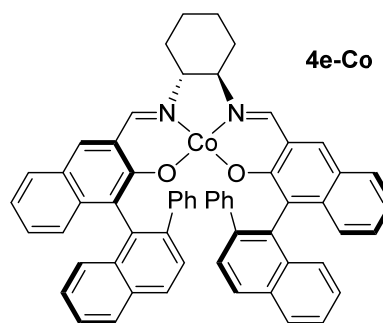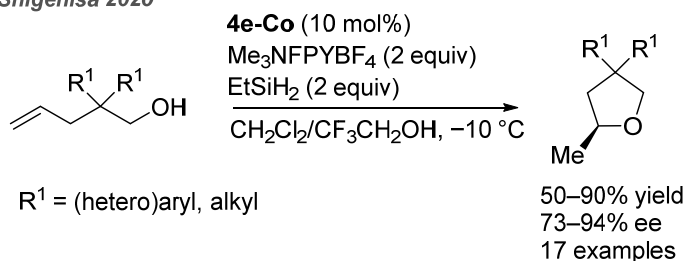
Figure 11. Co-salen-catalyzed asymmetric hydroalkoxylation of vinylic and homoallylic alcohols. ee = enantiomeric excess.

Last year, Shigehisa and co-workers also explored the structural effect of chiral cobalt salen catalysts on their previously developed cyclohydroalkoxylation methodology of unactivated alkenes (Figure 11, bottom) [89]. They identified the chiral and bulky binaphtyl ligands as optimal for the reaction of *gem*-disubstituted alkenols bearing terminal olefin, leading to the formation of various 5-membered rings in good yields and with moderate-to-high enantioinduction. Surprisingly, the authors also demonstrated that the sense and degree of enantioselectivity highly depend on the steric hindrance of the silane derivative. Indeed, the cyclization of 2,2-diphenylpent-4-en-1-ol affords mostly the (*S*)-enantiomer and the (*R*)-enantiomer of the cyclic ether with EtSiH$_2$ and (Me$_2$SiH)$_2$O, respectively. This silane-controlled enantiodivergence was experimentally and theoretically investigated and suggests that two competing selective mechanisms are operating involving respectively an alkylcobalt(III) and (IV) intermediate in the selective-determining step. The relative contribution of a radical chain reaction to these steps appears to depend on the silane controlled-concentration of a diffused carbon-centered radical.

4.2. Hydroamination

In 2014, taking advantage of the cobalt-based catalytic system developed for alkene hydroalkoxylation (vide supra), the Shigehisa group reported the intramolecular hydroamidation of aminoalkenes catalyzed by the same catalytic system (Figure 12) [90]. The authors proved again the impressive substrate scope and functional group tolerance of the reaction, affording 3- to 7-membered ring derivatives in good to excellent yields from *N*-protected amines tethered to mono- and 1,1′-disubstituted alkenes. When competitive hydroamidation vs. hydroalkoxylation can occur, it is worth noting that hydroalkoxylation with free alcohol was favored. The selectivity can be switched with appropriated protecting group on the alcohol, e.g., an acetyl (Ac) group, whereas MOM or TMS resulted in a mixture of C–N and C–O bond formations. Notably, the suitable protecting groups on the nitrogen atom are highly electron-withdrawing groups (Ac, Bz, Cbz, Boc, Ns, Ts, TFA), whereas substrates with free or benzyl (Bn) protected amine are not tolerated. In this respect, the authors show that the Co catalyst system strongly activates the olefin to react with weakly nucleophilic nitrogen atoms. When applying the same methodology to the cyclization of alkenyl guanidines bearing typical *N*-protecting groups, various five-, six- and even seven- to eight-membered rings guanidines were efficiently obtained [91]. These transformations likely operate via a cobalt-hydride hydrogen atom transfer and a radical-polar crossover similarly to the C–O bond formation methodologies described above.
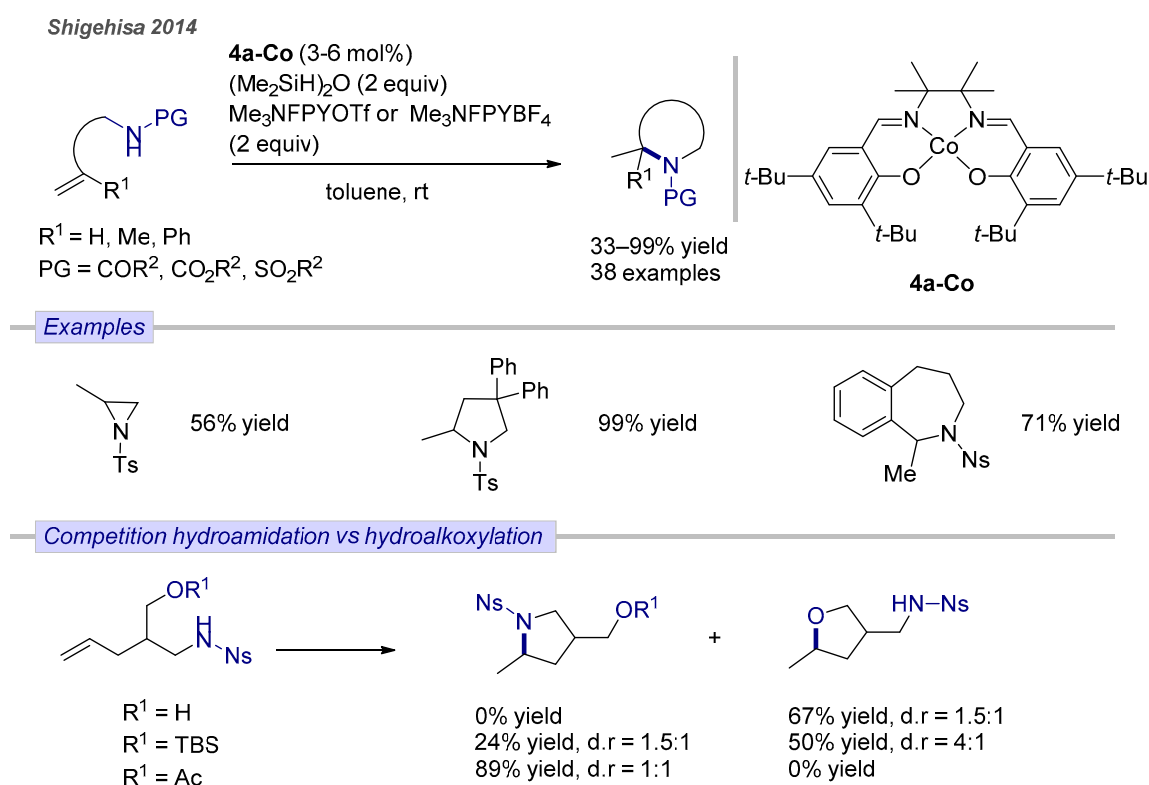
Figure 12. Cobalt-salen promoted cyclohydroamidation of *N*-protected amines tethered to mono- and 1,1′-disubstituted alkenes. rt = room temperature, d.r = diasteromeric ratio.

Based on the idea that the facile cleavage of weak N–N single bonds could deliver the free amines, the group of Akai and Yahata exploited the ability of the cobalt-Schiff base/*N*-fluorotrimethylpyridinium salts/hydrosilane combination to promote the Markovnikov selective hydroamination of benzotriazoles as amine surrogates and terminal aliphatic leading to N^2-alkylated benzotriazoles (Figure 13) [92]. In this study, racemic cobalt **4f-Co** along with PhSiH$_3$ gave the best performance in terms of yields and regioselectivity. The substrates' scope revealed the high chemoselectivity of the reaction with a wide range of

functional groups (protected alcohols, silyls, esters, halogens) tolerated on both reaction partners. The reduction of the N–N bonds providing the free amines was demonstrated through zinc-mediated reduction in acidic media (Figure 13). Although the enantioinduction was poor using enantiopure (*R,R*)-**4f-Co**, this demonstrates that the catalyst interacts with the substrate during the C–N bond formation and offers great promise for the future development of a highly enantioselective Markovnikov cobalt-catalyzed hydroamination reaction. Based on control experiments, the authors postulated that the reaction mechanism proceeds in a similar way as the hydroalkoxylation, through the formation of a cationic alkylcobalt(IV) intermediate by a metal-hydride HAT and radical-polar crossover process. Subsequent S_N2-like displacement with silylated benzotriazole substrate affords the hydroamination product and regenerates the Co(II) catalyst. Notably, through this synthetic strategy, the authors also reported access to a large range of 2,5-disubstituted tetrazoles (18 examples, 43–83% yields) from the reaction of 5-substituted tetrazoles and unactivated aliphatic alkenes [93]. Using enantiopure cobalt catalysts, a promising asymmetric version toward enantioenriched 2,5-disubstituted tetrazoles with ee's up to 66% was reported.
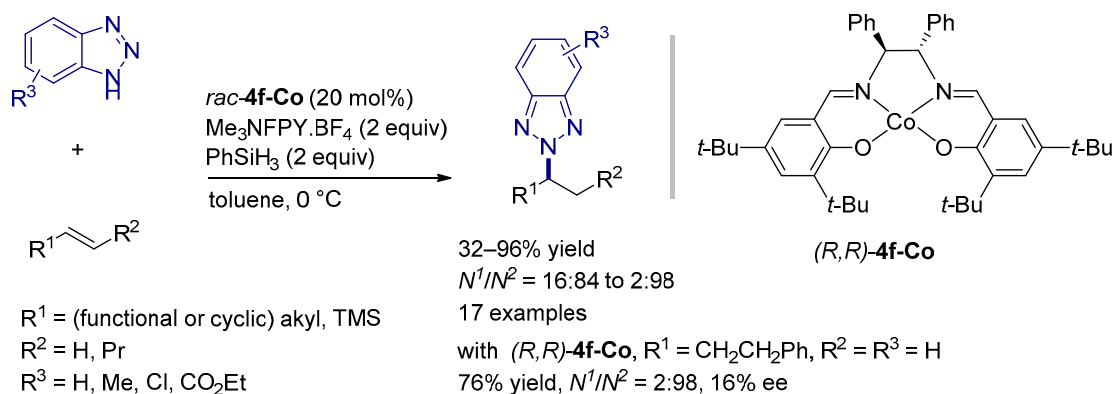
Figure 13. Cobalt-salen promoted Markovnikov selective hydroamination of benzotriazoles and terminal aliphatic and conversion of N^2-alkylated benzotriazoles products into primary amines. rt = room temperature, ee = enantiomeric excess.

Based on the similar concept of promoting formal alkene hydroamination via MHAT and through an undirect pathway requiring a N–N bond cleavage step, the group of Lu recently reported a Co-catalyzed hydrohydrazidation of alkenes using diazo compounds in the presence of *NNN*-tridentate ligand and PhSiH$_3$ [94]. With a large substrate scope, the efficiency and the high tolerance towards various functional groups were well-established (42 examples, 50–95% yields). Coupled to a Zn-mediated N–N single bond reduction under acidic conditions followed by Boc-, Bz-protection or *N*-alkylation, a three steps protocol afforded various secondary amines (29 examples, 35–75% yields). Remarkably, when an enantiopure ligand was introduced, hydroamination products were obtained with good enantioselectivity (89:11 to 93:7 enantiomeric ratio (er)). It is worth noting that a similar protocol was successfully applied to sequential hydrogenation/hydrazidation of aliphatic terminal alkynes [95].

In 2019, in order to widen the application scope of this cobalt-catalyzed alkene hydrofunctionalization methodology, the Zhu research group proposed to use an additional

catalytic oxidant for a better redox matching during the radical-polar crossover process that converts the organocobalt(III) species (resulting from metal-hydride HAT of alkene followed by cage collapse) into the cationic organocobalt(IV) intermediates [96,97]. By evaluating the electrochemical properties of **4a-Co** and its cyclohexenediamine-derivative as well as a model alkylcobalt(III)-salen complex, it was hypothesized that the facile reductive quenching of the excited state of $Ru(bpy)^{3+}$ by organocobalt(III) species should lead to the formation of the key Co(IV) intermediate and that subsequent nucleophilic trapping should give the desired Markovnikov product. The stoichiometric presence of a two-electron oxidant, such as *N*-fluoro pyridinium salts, should trigger the regeneration of Ru(III) and Co(III) species. This analytic-driven approach has allowed the efficient development of a novel methodology for the Markovnikov intermolecular hydrofunctionalization of vinyl(hetero)arenes and a variety of *N*-heterocycles (indazoles, imidazoles, pyrazoles, carbazoles) and sulfonamides by a light-mediated cobalt-ruthenium dual catalysis as illustrated in Figure 14. Mechanistic investigations support the postulated photochemical oxidation of alkylcobalt(III) species. This successful merger of a photoredox cycle with Co-mediated HAT should open the door for further interesting developments in the rich chemistry of CoH-mediated oxidative hydrofunctionalization reaction.
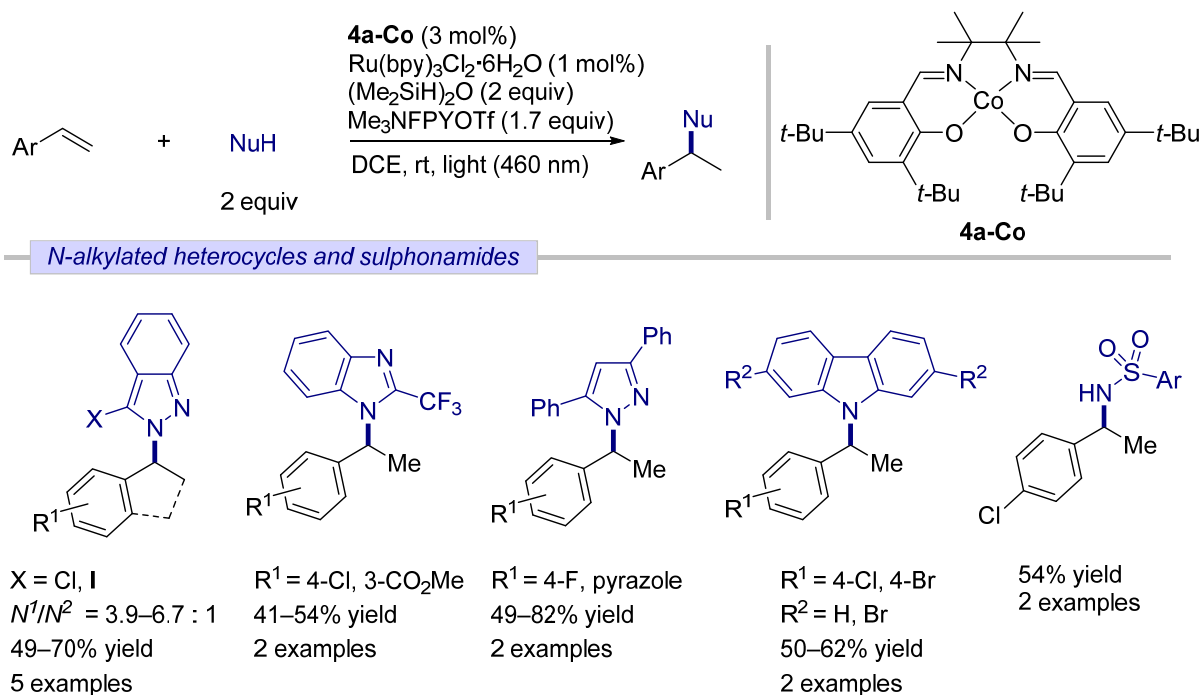
Figure 14. Markovnikov intermolecular hydroamination of *N*-heterocycles and sulfonamides and styrenes based on visible-light-mediated Co/Ru dual catalysis. rt = room temperature.

In 2018, with the aim of developing a Co-catalyzed direct hydroamination protocol with primary amines (and oxidant-free) and inspired by their previous Fe-catalyzed cyclohydroamination, [64] Ujaque, Lledós and Hannedouche developed a β-diketiminatocobalt(II) complex to promote the *exo*-cyclization of unprotected aminoalkenes under mild conditions (Figure 15) [98,99]. This report was the first example of cobalt-catalyzed hydroamination of primary amines. It is worth mentioning that contrary to the Fe catalyst [64], a phenyl ring at the terminal position of the alkene was necessary to prevent alkene isomerization as a dominant pathway. This protocol allows the formation and isolation of diverse *gem*-disubstituted pyrrolidines and piperidines in good-to-high yields. However, it was unsuccessful for the cyclization of amines tethered to trisubstituted alkenes or substrates unbiased toward cyclization but suitable for primary amines bearing dimethyl-substituted

allene or alkyne functionality. Joint experimental and theoretical investigations of the reaction mechanism suggested that the reaction proceeds through a nucleophilic attack of the amido group of monomeric cobalt(II) amidoalkene-aminoalkene adduct intermediate to the non-coordinated pendant alkene as the rate-determining step; followed by a rapid proton transfer from the coordinated substrate, which results in the cyclized adduct. This novel stepwise non-insertive mechanism in the field of alkene hydroamination is distinct from the stepwise insertive mechanism encountered in the Fe-catalyzed hydroamination of primary amines tethered to olefins.

Ujaque, Lledós and Hannedouche 2018
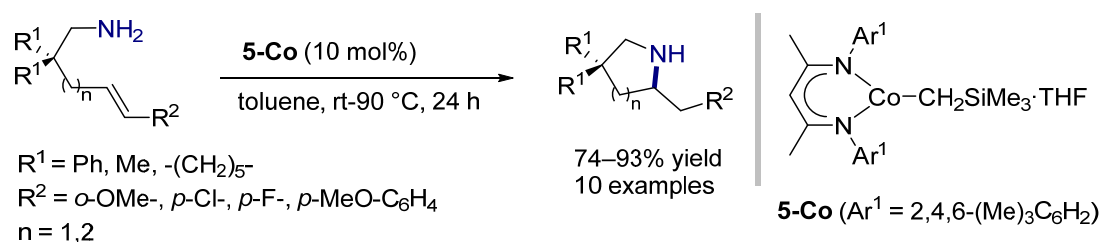
Figure 15. Well-defined β-diketiminatocobalt(II) alkyl-catalyzed hydroamination of primary amines tethered to alkenes.

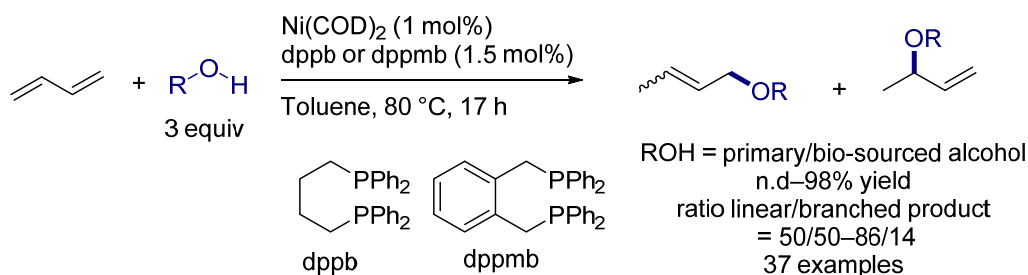## 5. Nickel

5.1. Hydroalkoxylation

The first example of Ni-catalyzed alkene hydroalkoxylation was reported by Suisse and Sauthier et al. in 2013 (Figure 16) [100]. They observed that the hydroalkoxylation of 1,3-butadiene with methanol, ethanol or benzylic alcohol promoted by a $Ni(acac)_2$/1,4-bis(diphenylphosphino)butane (dppb) in the presence of $NaBH_4$ affords alkylbutenyl ethers with high selectivity. In 2016, the same group performed an interesting optimization of this catalytic system to further improve the selectivities and proposed the use of 1,2-bis(diphenylphosphinomethyl)benzene (dppmb) as an alternative to 1,4-bis(diphenylphosphino)butane (dppb) (Figure 16). Under optimized catalytic system, a large range of substituted dienes was performed but a decrease of reactivity was observed compared to butadiene. However, this study proved the efficiency of the catalytic system under mild conditions for a large range of primary alcohols including bio-sourced alcohols [101]. A joint experimental and computational mechanistic study of the dppb- and dppmb-ligated nickel-catalyzed hydroalkoxylation reaction of butadiene discards the involvement of Ni-H species and shows that the formation of Ni-allyl species are likely intermediates accessible from direct protonation of the ligated Ni(0)/butadiene species [102]. The methodology was further applied to the hydroalkoxylation of butadiene with glycerol to obtain glyceryl-butenylethers (GBE) [103,104].

In 2019, Mazet and co-workers developed a highly regioselective Ni-catalyzed hydroalkoxylation of 2-(hetero)aryl-substituted 1,3-dienes with primary alcohols under mild conditions (Figure 17) [105]. An excellent Markovnikov selectivity up to >20:1 resulting from a 3,4-addition was achieved by using the achiral dicyclohexylphosphinooxazoline ligand (Cy-PHOX) (Figure 17). The optimized protocol provides an access to a broad range of structurally diverse allylic ethers and tolerates a number of sensitive functional groups, such as halogens, nitriles, esters or pyridine or *N*-methyl imidazole. Isotopic labeling experiments have shown that the transformation is reversible and expected to involve Ni-π-allyl species reminiscent of those observed in the related hydroamination reactions (vide infra). Encouraging results in the development of an asymmetric version of this process were observed with the use of a ferrocenyl-based enantiopure phosphinooxazoline ligand.

Suisse and Sauthier 2013, 2016

Figure 16. Nickel-catalyzed intermolecular hydroalkoxylation of butadiene and alcohols. n.d = not determined.

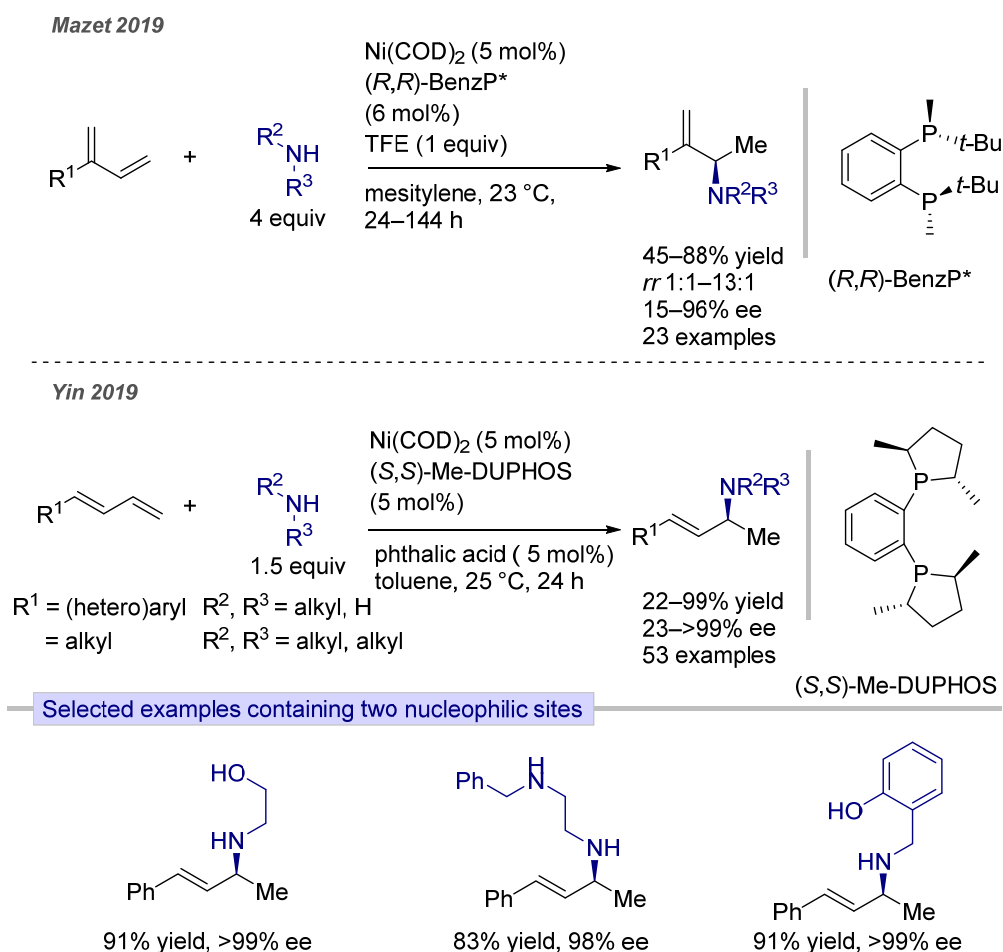*Mazet 2019*
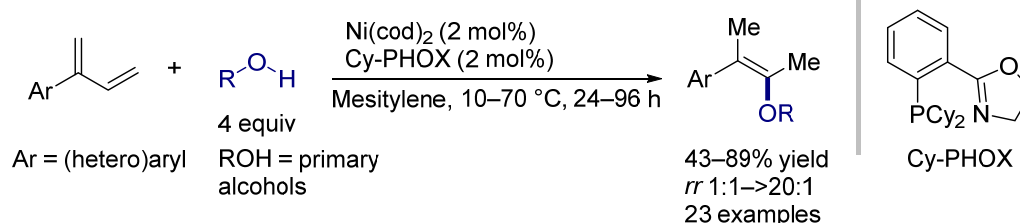
Figure 17. Regioselective Ni-catalyzed hydroalkoxylation of 2-(hetero)aryl-substituted 1,3-dienes and primary alcohols. *rr* = regioselectivity defined as ratio 3,4-addition product vs. 1,4-addition products.

5.2. Hydroamination

Early studies have demonstrated the ability of Ni-based system to catalytically promote the hydroamination of 1,3-dienes [106–108]. In 2019, inspired by the work of Hartwig on cyclic dienes [105], the group of Mazet reported a regio- and enantioselective Ni-catalyzed intermolecular hydroamination of 2-substituted 1,3-dienes with primary and secondary amines under mild conditions using a catalytic combination of Ni(COD)$_2$ and enantiopure biphosphine (*R,R*)-BenzP* ligand and trifluoroethanol (TFE) as an additive (Figure 18, top) [109]. The method is broadly applicable, highly regio-, chemo-, and enantioselective for 2-(hetero)aryl-substituted 1,3-dienes and primary amines, and provides direct access to valuable enantioenriched allylic secondary amines by selective 3,4-addition. However, the reaction, which is compatible with a range of functional groups, appears more challenging for 2-alkyl-substituted 1,3-dienes or secondary amines leading to a significant decrease in yield and regioselectivity, despite a high enantioinduction. In-depth mechanistic investigations highlight that the C–N bond formation is rate-limiting and proceeds by an outer-sphere nucleophilic addition on a Ni-π-allyl species assigned as the catalytic resting state. In contrast to hydroalkoxylation described in Figure 17, this step is irreversible.

The same year, a novel biphosphine ligated nickel-catalyzed asymmetric hydroamination of monosubstituted 1,3-dienes using a Brønsted acid as cocatalyst was established by the group of Yin (Figure 18, bottom) [110]. By using a catalytic combination of Ni(COD)$_2$, enantiopure rigid ligand (*S,S*)-Me-DuPhos and phthalic acid as Brønsted acid, a wide series of primary and secondary amines could be selectively added to 4-aryl and 4-alkyl-substituted 1,3-dienes affording enantioenriched functionalized allylic amines in yields and with enantioselectivity up to 99%. The choice of chiral biphosphine ligand and the use of an appropriate Brønsted acid as cocatalyst were key to the success of this hydroamination reaction. A preliminary mechanistic study indicates that the C–N bond-forming step is, in this case reversible leading to racemization over time for the reaction of secondary amines but not for primary amines. The methodology has a good functional group tolerance and exhibits good chemoselectivity with respect to amines bearing two different nucleophilic sites but is unsuitable to the reaction of disubstituted 1,3-dienes.

Mazet 2019

Yin 2019

Selected examples containing two nucleophilic sites

91% yield, >99% ee 83% yield, 98% ee 91% yield, >99% ee

Figure 18. Regioselective Ni-catalyzed hydroamination of 2- and 1-substituted 1,3-dienes and primary and secondary amines. *rr* = regioselectivity defined as ratio 3,4-addition product vs. 1,4-addition products, ee = enantiomeric excess.

Although great progress has been made in the Ni-catalyzed hydroamination of 1,3-dienes and 1,2-dienes [111], there are only a few reports on the development of nickel-based catalysts for the regioselective hydroamination of an unactivated terminal and more challenging internal alkenes [112]. In 2020, the group of Hong made a breakthrough in this domain by reporting an efficient Ni-H-based system having the ability to promote a proximal-selective hydroamination of unactivated alkenes tethered to a bidentate directing group (Figure 19) [113]. Indeed, the combination of $Ni(acac)_2/(EtO)_2MeSiH$ in the presence of electrophilic hydroxylamine esters as amine transfer agent provides a useful synthetic method for the conversion of mono-, di- and trisubstituted alkenes tethered to amide-linked aminoquinoline or to amine-derived picolinamides to structurally diverse and functionalized β- and γ-amino acid building blocks in moderate to good yields. It is interesting to note that both (*E*) and (*Z*)-alkenes are compatible as well as mono- and dialkyl-substituted amine transfer agent. The strong bidentate coordination ability of the directing groups to the Ni–H species is crucial to promote and regiocontrol the challenging migratory-insertion of the Ni–H species into the substituted alkene. In-depth kinetic studies and DFT calculations suggest that this step is rate-limiting.

Hong 2020
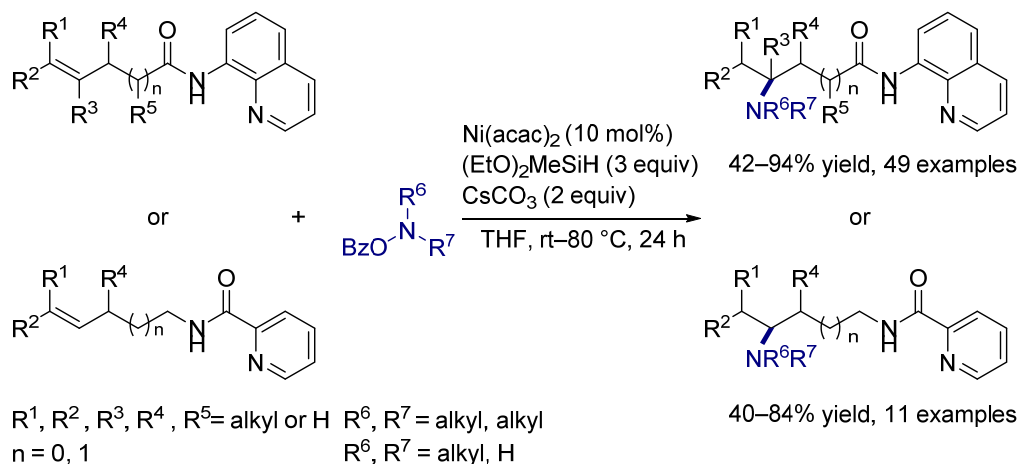
Figure 19. Regiocontrolled Ni-catalyzed hydroamination of alkenes tethered to amide linked amino-quinoline or to amine-derived picolinamides. rt = room temperature.

6. Copper

6.1. Hydroalkoxylation

In 2015, the group of Sawamura reported the cyclohydroalkoxylation of *gem*-disubstituted alkenols catalyzed by a mesitylcopper(I)/Xantphos (**L$_0$**) (Figure 21) system according to a different activation mode from other copper Lewis-acid catalysts previously reported [114–116] for alkene hydroalkoxylation (Figure 20) [117]. In this system, the basic copper (pre)catalyst activates the alcohol functionality of the substrate to form an alkoxycopper(I) species that can further insert into the terminal alkene and leads after homolysis to the desired cyclic ether. Ligand screening identified Xantphos (**L$_0$**) with a large bite angle as the most efficient ligand for the cyclization of 2,2-diphenyl-4-penten-1-ol. The protocol was reported for the hydroalkoxylation of primary and secondary *gem*-disubstituted alkenols, but not for substrates unbiased for cyclization andwas inefficient for the transformation of alcohol tethered to 1,2-disubstituted alkene. Preliminary studies on the development of an asymmetric version of this protocol revealed that, among the chiral ligand screened, enantiopur (*R*)-DTBM-SEGPHOS (**L$_3$**) (Figure 21) ligand could afford 2-methyl-4,4-diphenyltetrahydrofuran with 71% ee under slight reaction conditions modifications but in low yield. This report was the first example of metal-catalyzed enantioselective cyclohydroalkoxylation of unactivated alkenes.

Sawamura 2015
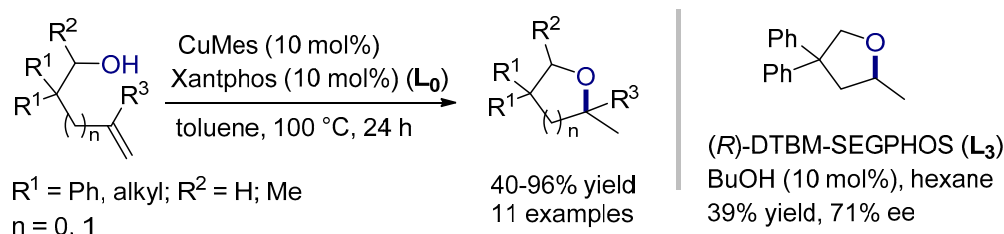
Figure 20. Cu(I)-Xantphos-catalyzed cyclohydroalkoxylation of alkenols.
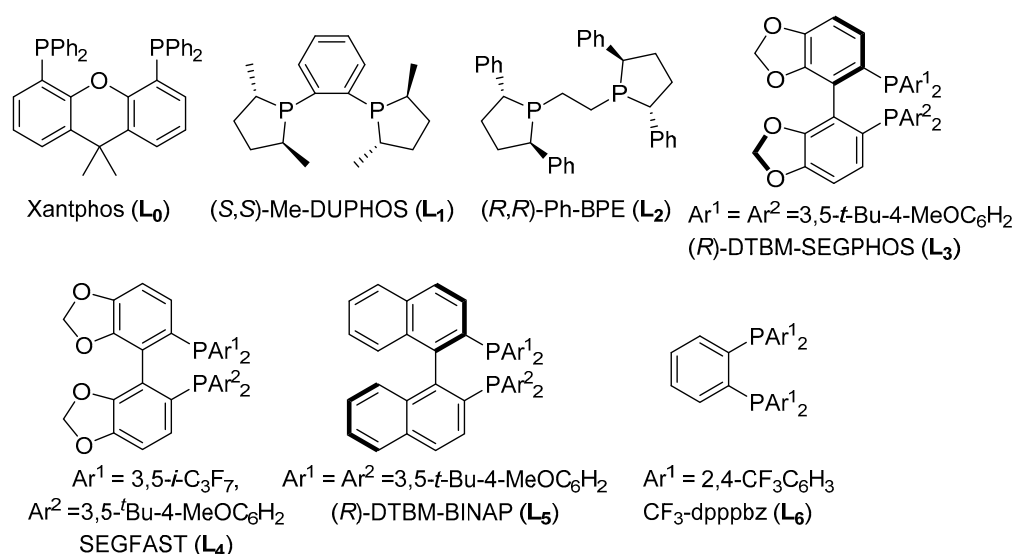
Figure 21. Bidentate biphosphine ligands used in Cu-catalyzed hydrofunctionalization reactions.

Last year, inspired by their previous works on copper(II)-catalyzed enantioselective carboetherifications of alkenols [118–121], the group of Chemler reported the enantioselective cyclohydroalkoxylation of a range of aliphatic 4- and 5-alkenols catalyzed by chiral copper(II) bis(oxazoline) (Figure 22 [122]. In the presence of an oxidant and an H-atom donor, the Cu(OTf)$_2$/(S,S)-*i*-Pr-Box (**L$_7$**) or (S,S)-Ph-Box (**L$_8$**) system is indeed an efficient system to access enantioenriched α-chiral substituted tetrahydrofurans, phthalans, isochromans and morpholine from primary and tertiary alcohols tethered to the terminal, 1,1- and 1,2-disubstituted alkenes as illustrated in Figure 22. This system is limited to (*E*)-alkenes as (*Z*)-isomers are less selective, affords higher enantioinduction for tertiary alkenols than primary alkenols and is unreactive for phenols. Isotopic labeling experiments and previous works are in favor of a polar/radical mechanism implying *cis*-oxycupration of the alkene followed by homolysis of the subsequent σ-Cu–C bond and H-atom transfer. Oxidation of the Cu(I) to Cu(II) species completes the catalytical cycle.
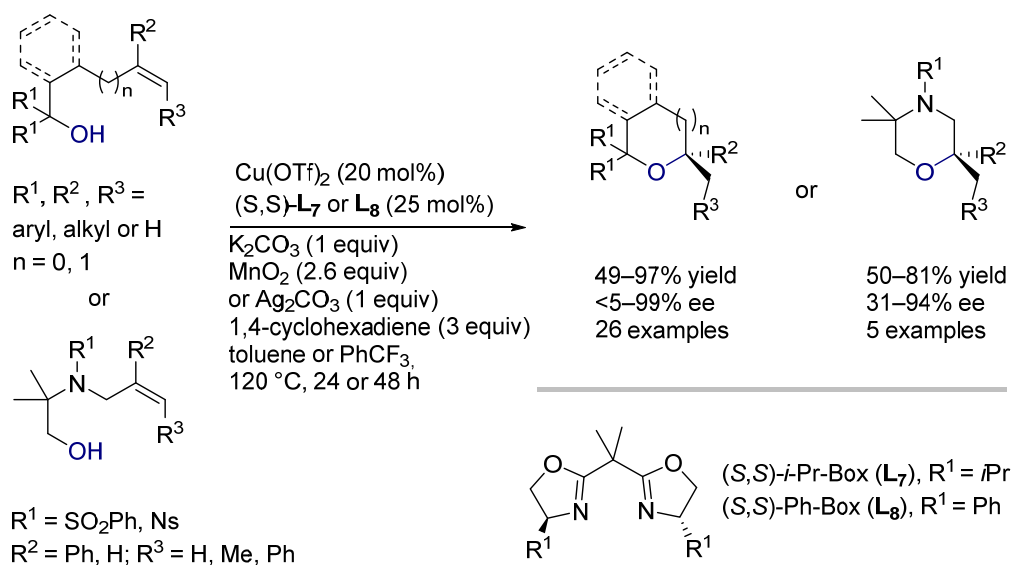
Figure 22. Cu(II)-bis(oxazoline)-catalyzed enantioselective cyclohydroalkoxylation of 4- and 5-alkenols. ee = enantiomeric excess.

6.2. Hydroamination

Earlier works in the field have highlighted the potential of copper catalysis to promote inter- and intramolecular hydroamination of unactivated alkenes and sulfonamides [123–125], or less common protecting group-free primary amines [126,127]. In 2017, the group of Monnier and Taillefer disclosed the first report of copper-catalyzed intermolecular hydroamination of terminal allenes and cyclic secondary amines or anilines using a ligand-free copper(II) triflate salt as precatalyst (Figure 23) [128–130]. This method is highly regio- and stereoselective affording exclusively the corresponding linear (*E*)-allylamines in moderate-to-excellent yields and is compatible with various functional groups (ethers, free tertiary alcohols, halogens, imides) on both partners. A joint experimental and theoretical mechanistic study rationalizes the reaction selectivity in favor of the linear (*E*)-allylamine product and supports a cationic Cu(I) species as the catalytically active species [131]. This study allows the extension of this protocol to the reaction of various functionalized allenamides, *N*-allenyl-carbamates, -(1,2)-azoles and -(1,3)-azoles under milder conditions using Cu(NCMe)$_4$(PF$_6$) [132] as precatalyst (Figure 23) [128,133]. More recently, it was demonstrated that the protocol using Cu(NCMe)$_4$(PF$_6$) was also efficient for the hydroamination of *N*-allenyl-sulfonamides and trifluoromethyl-containing α-allenyl-α-aminocarboxylates and α-allenyl-α-aminophosphonate with similar regio- and stereoselectivity [134,135].
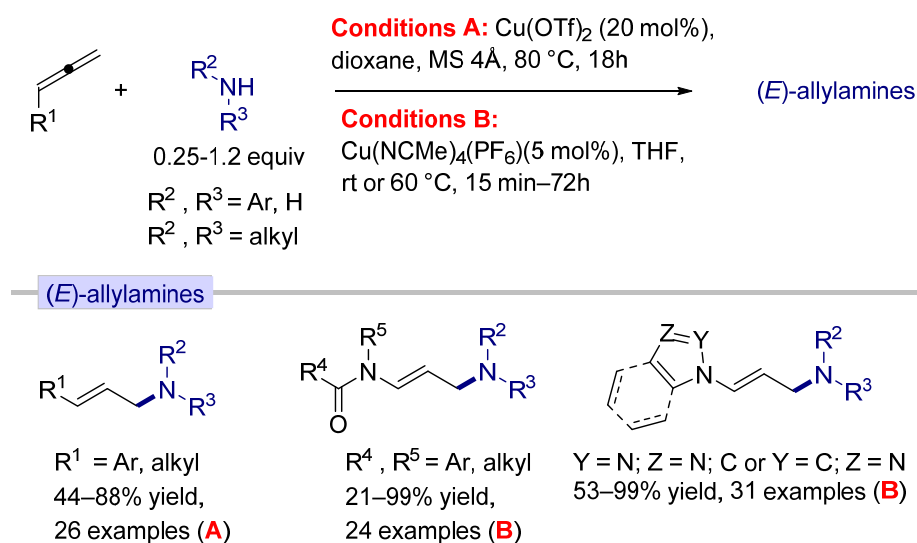
Figure 23. Regio- and stereoselective Cu(II)-catalyzed intermolecular hydroamination of terminal allenes. rt = room temperature.

In 2013, an astounding breakthrough based on an innovative strategy was independently but contemporaneously reported by the groups of Hirano, Miura [136] and Buchwald [137] for the highly regio- and enantioselective intermolecular hydroamination of arylalkenes with exclusive Markovnikov selectivity (Figure 24) [138,139]. This strategy exploits the well-known phosphine-ligated copper-hydride chemistry of reduction [140,141] and the electrophilic character of hydroxylamine esters [142] to propose an original umpolung amination approach for the C–N bond formation. Both reports disclose that the combination of a Cu(I) or (II) salt and a chiral biphosphine ligand in the presence of a reducing silane agent provides highly efficient catalytic systems for the regio- and enantioselective hydroamination of styrene derivatives and *O*-benzoylhydroxylamines, affording Markovnikov addition products in good-to-excellent yields with a similarly high level of enantioselectivity (Figure 24). The Miura and Hirano combination ((*S*,*S*)-Me-Duphos (**L₁**) or (*R*,*R*)-Ph-BPE (**L₂**) (Figure 21))/CuCl/diethoxymethylsilane/LiOtBu) can be applied to functionalized styrenes and *trans*-β-substituted styrenes but is unsuitable

for *cis*-β-substituted styrenes and terminal alkenes, although it allows the conversion of strained aza and oxa-bicyclic alkenes [132,143]. The original Buchwald ((*R*)-DTBM-SEGPHOS (**L₃**) (Figure 21)/Cu(OAc)₂/HSiMe(OEt)₂) has a broader scope, providing the enantioenriched tertiary amines for functionalized styrenes, *cis*- and *trans*-β-substituted and β,β-disubstituted styrenes [133]. Furthermore, using the racemic version of this copper system, terminal and linear aliphatic olefins afford amines in high yields with anti-Markovnikov regioselectivity.
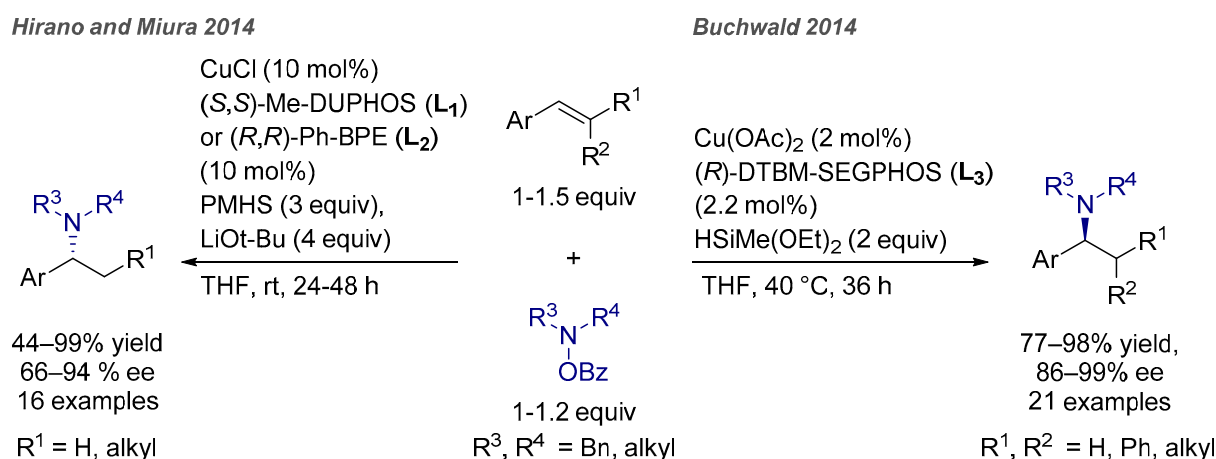
Figure 24. Regio- and enantioselective CuH-catalyzed hydroamination of arylalkenes with hydroxylamine esters. ee = enantiomeric excess.

Detailed mechanistic studies conducted on the C–N bond formation of styrenes and *O*-benzoyl-*N*,*N*-dialkyl-hydroxylamine [144], and completed by computational investigations [145] proposed that the reaction proceeds by (1) in situ formation of catalytically competent and monomeric **L₃**Cu(I) –H (in a putative equilibrium with its dimer or higher-order species or aggregates) from the ligand **L₃**, Cu(OAc)₂ and the hydrosilane reagent (2) irreversible, enantio-determining and regioselective alkene 2,1-migratory insertion into the Cu–H σ-bond (3) subsequent, stereoretentive electrophilic amination of the ensuing insertive copper species by the amine reagent which leads to C–N bond formation, liberation of hydroamination product and generation of **L₃**Cu(I)–OBz as the catalyst resting state (4) rate-determining transmetalation between **L₃**Cu(I)–OBz and the hydrosilane regenerates **L₃**Cu(I)–H. Formation of a less sterically congested insertive copper species (resulting from migratory-insertion) and electronic stabilization by the adjacent aryl group may account for the anti-Markovnikov and Markovnikov regioselectivity noticed for linear olefins and styrene derivatives respectively. For terminal (and internal) olefin, the hydrocupration step is likely rate-limiting. As suggested by DFT calculations, the superior efficiency of the bulky DTBM-SEGPHOS (**L₃**) ligand over other biphosphine ligand originates primarily from a better stabilization of the hydrocupration transition state due to greater superior dispersion interactions from the *tert*-butyl substituent of the phosphine and the alkyl substituent of the olefin [146]. The understanding of the substrate-ligand interactions was exploited to increase the activity of the CuH catalyst through the design of SEGFAST ligand (**L₄**) (Figure 21) [147]. Indeed, this ligand affords a 62-fold rate increase compared to **L₃** in the formal hydroamination of terminal aliphatic olefins and *O*-benzoyl-*N*,*N*-dibenzyl-hydroxylamine. Both 3,5-*i*-C₃F₇ and 3,5-*t*-Bu-4-MeOC₆H₂ substituents of the ligand are essential to reach the appropriate balance between catalyst reactivity and stability.

Over the years, this biphosphine CuH-methodology has been impressively extended to a plethora of class of unactivated and less activated alkenes besides styrenes and linear terminal alkenes including a range of various *trans*-1,2-and 1,1′-disubstituted alkenes, cyclic *cis*-1,2- disubstituted and even strained alkenes as summarized in Figures 25 and 26, delivering the chiral tertiary amines at an impressively high level of enantioinduction.

It is indeed efficient for the regio- and enantiocontrolled hydroamination of vinylsilanes [148], 1,1-disubstitued alkenes [149], symmetric [150] or unsymmetrical (*E*)-1,2-dialkylsubstituted alkenes [151] (including the feedstock olefin, (*E*)-2-butene [146]), alkenyl 1,8-diaminonaphthyl boronates [152], vinylphosphine boranes [153], 1-trifluoromethylalkenes [154], enamines [155], *N*-protected γ-substituted allylic amines [156], unprotected allylic alcohols [157] delivering a range of structurally diverse β-chiral, α- and β-functionalized tertiary amines in moderate-to-high enantiopurity as privileged building blocks (Figure 25). Although minimal alteration of the initial reaction conditions using the DTBM-SEGPHOS ligand (**L₃**) as privileged ancillary ligand is usually required, structural optimization of the amine transfer agent, hydrosilane, ligand and substrate or use of additional monodentate phosphine ligand (PPh₃, P(*p*-tolyl)₃), proton source (*t*BuOH) or specific external bases (LiOtBu, CsOAc) was needed in some cases to broaden the scope to new compound families and/or overall improve the process efficiency. For instance, the use of an electron-enriched amine transfer agent (such as *p*-NMe₂C₆H₄CO₂NR¹R²) instead of the original BzONR¹R² was crucial for the productive enantioselective transformation of the challenging unactivated internal alkenes [146], vinylphosphine boranes [149], enamines [151], allylic amines and alcohols [152,153]. This electronic effect may result in a better ability to restore the competent active Cu(I)–H in the rate-determing transmetation step for the catalytic cycle and a dismished non-productive deterioration of the electrophilic amine by the catalyst. In another example, the judicious choice of the ligand (*R*)-**L₅** (Figure 21) and additional base CsOAc was key to suppress the undesired β-F elimination side-reaction from the alkylcopper intermediate for the formation of enantiopur α-trifluoromethylamines of great interest in medicinal chemistry [150]. Additionally, the nature of the protecting group on the nitrogen or oxygen functionality attached at the (homo)allylic position of the internal alkenes significantly improves the reaction efficiency by either enabling the hydrocupration, preventing the detrimental β-H elimination or electronically controlling the regioselectivity [147,152]. In some cases, the addition of a stoichiometric amount of *t*-BuOH and/or catalytic amount of PPh₃ to the reaction medium could enhance the reaction rate and improve the yield of C–N bond formation product, as is the case in the formation of enantioenriched *N*-arylamines [158], by suppression undesired reduction pathways [147,152]. This methodology could also be impressively extended to the asymmetric synthesis of three and five-membered *N*-heterocycles, such as aziridines or α-(hetero)arylpyrrolidines or six- to nine membered benzo-fused analogues by intramolecular cyclization of hydroxylamine ester derivatives (not shown in Figure 25) [159,160].

Although most of the studies on internal alkenes were pursued on (*E*)-isomers [161], this protocol was recently successfully extended to *cis*-1,2-disubstituted alkenes known as challenging and problematic alkene partners [162]. Indeed, the CuH-methodology with (*R*)-DTBM-SEGPHOS (**L₃**) or (*R*,*R*)-Ph-BPE (**L₂**) ligand (Figure 21) was efficiently applied to the regio- and enantioselective hydroamination of various substituted 2H-chromenes [163], 1,2-dihydroquinolines [164] and benzofurans [165] to access a series of 4-aminochromanes, 4-aminotetrahydroquinolines and *N*,*N*-dibenzylaminophenols respectively as important key building blocks (Figure 26). The latter products arise from CuH-promoted ring-opening of the benzofuran scaffold and subsequent regio- and enantio-controlled hydroamination of the resulting arylalkene. Key to the success of these applications was the fine-tuning of the electrophilic amine partner or the use of additional phosphine ligand. Strained alkenes are also a class of alkenes that have been successfully converted into useful N-based compounds (Figure 26). Indeed, CuH-catalyzed regioselective ring-opening hydroamination of 2-aryl and -alkyl-substituted methylenecyclopropanes and *O*-benzoylhydroxylamines afford the corresponding homoallylic amines via ring cleavage at the more congested position [166]. Ligand screening reveals a notable ligand effect and leads to the identification of CF₃-dppbz (**L₆**) (Figure 21) as the more efficient bidentate phosphine for this process (Figure 26). In general, unactivated trisubstituted alkenes are an extremely challenging class of substrates for CuH-promoted hydroamination reaction. A strategy to achieve such reactivity is to rely on the release of the ring strain energy of stained trisubstituted

olefins. Early last year, the group of Buchwald reported the diastereo- and enantioselective CuH-catalyzed hydroamination of 1-aryl and alkyl-substituted cyclobutenes, and 1-phenyl, 1-alkyl, 1-silyl substituted cyclopropenes leading to the C–N bond formation with different regioselectivity according to the substitution and ring size (Figure 26) [167]. Markovnikov regioselectivity was noticed for 1-arylcyclobutenes while anti-Markovnikov regioselectivity was observed for all other substrates.

Buchwald, Miura, Hartwig and Somfai 2014-2019
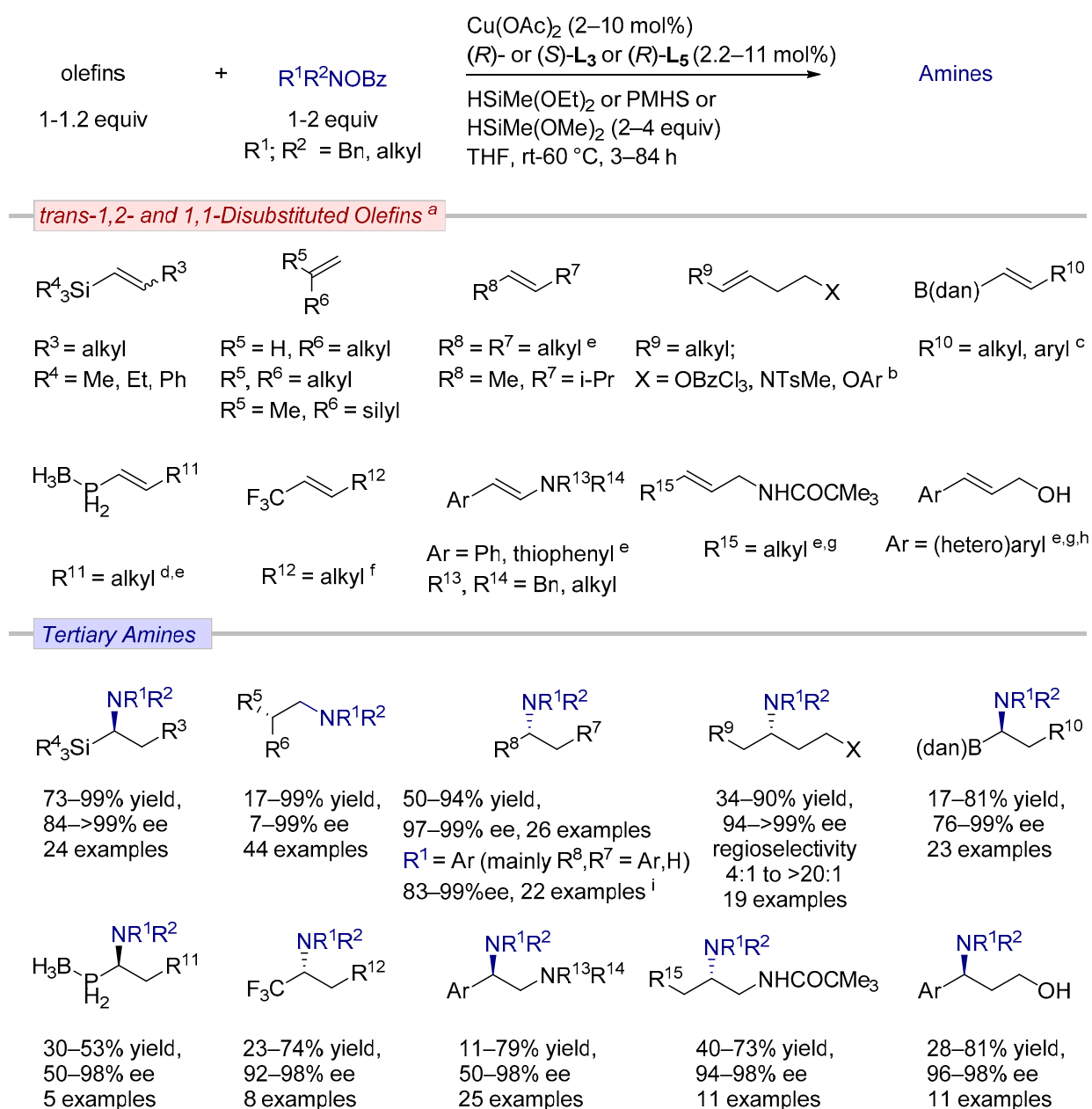
Figure 25. Regio- and enantioselective biphosphine·CuH-catalyzed hydroamination of 1,2-*trans* and 1,1′-disubstituted alkene derivatives. [a] all reactions run with Cu(OAc)$_2$, (R) or (S)-**L$_3$**, R^{1}R^{2}NOBz (R^1; R^2 = Bn, alkyl) in THF unless otherwise stated. [b] 10 mol% Cu(PPh$_3$)H. [c] with LiOtBu (4 equiv). [d] Cu(OAc)$_2$·H$_2$O (10 mol%) with LiOtBu (3 equiv) in CPME. [e] with p-NMe$_2$C$_6$H$_4$CO$_2$NR^{1}R^2. [f] Cu(OAc)$_2$·H$_2$O (10 mol%), (R)-**L$_5$**, CsOAc (2 equiv) in 1,4-dioxane. [g] (R)-CuCatMix* (Cu(OAc)$_2$/(R)-**L$_3$**/PPh$_3$ = 1/1.1/1.1. [h] in cyclohexane. [i] PPh$_3$ (6.0 mol%), t-BuOH (1.0 equiv). dan = 1,8-diamononaphthyl. rt = room temperature, ee = enantiomeric excess.

Buchwald, Miura, Wang, Zhang and You 2016, 2018-2020

Cu(OAc)$_2$ (2–10 mol%)
(R)- or *rac*-**L$_3$** or (R,R)-**L$_2$** or **L$_6$** (2.2–11 mol%)

olefins + R^{1}R^{2}NOBz $\xrightarrow{\text{HSiMe(OMe)}_2 \text{ or PMHS (3-5 equiv)}}$ Amines
1–5 equiv   1–2 equiv   THF, rt–45 °C, 4–6 h
(R^1; R^2 = Bn, alkyl)

Cyclic cis-1,2-Disubstituted and Strained Olefins [a]

R^3 = MeO, Aryl, NO$_2$, Cl, F [b,c]   R^6 = alkyl, halogen, (thio)ether, (thio)phenyl, [d]   R^8 = Me, Ph, MeO, MeS, Br, Cl,
R^4, R^5 = H, Ph, alkyl   R^7 = alkyl   MeO$_2$C [b]

R^9 = aryl, (CH$_2$)$_2$Ph [e]

R^{10} = (hetero)aryl, alkyl
R^{11} = H, alkyl
R^{12} = H, Ph, alkyl
n = 0,1 [f]

Tertiary Amines

50–88% yield,
66–99% ee
21 examples

45–97% yield,
82–93% ee
32 examples

18–66% yield,
37–94% ee
16 examples

53–99% yields
25 examples

R^{10} = (hetero)aryl
65–90% yield, d.r up to 29:1
9 examples

R^{10} = alkyl, SiMe$_2$Ph; n = 0,1
R^{10} = Ph, n = 0
58–92% yield, 38–99% ee
d.r >20:1, 11 examples

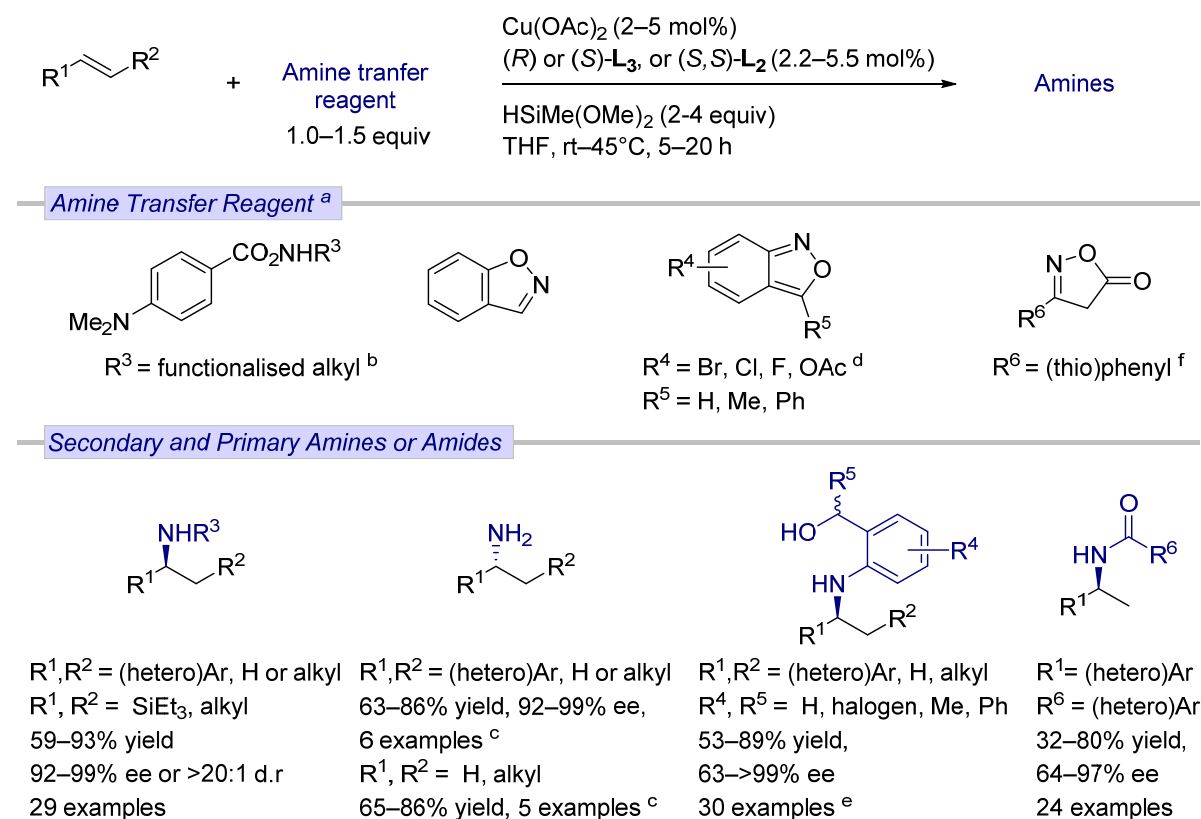**Figure 26.** Regio- and enantioselective biphosphine·CuH-catalyzed hydroamination of alkene derivatives and electrophilic amines. [a] all reactions run with Cu(OAc)$_2$, (R)-**L$_3$**, R^{1}R^{2}NOBz (R^1; R^2 = Bn, alkyl) in THF unless otherwise stated. [b] *p*-NMe$_2$C$_6$H$_4$CO$_2$NR^{1}R^2. [c] PPh$_3$ (5.5 mol%). [d] P(*p*-tolyl)$_3$ (4.4 mol%), (R,R)-Ph-BPE (**L$_2$**), AdCO$_2$NR^{1}R^2. [e] CF$_3$-dppbz (**L$_6$**) (10 mol%), LiO*t*Bu (4 equiv) in DCE. [f] 1,3,5-Me$_3$C$_6$H$_2$CO$_2$NR^{1}R^2 or BzONR^{1}R^2 or PivONR^{1}R^2. rt = room temperature, d.r = diasteromeric ratio, ee = enantiomeric excess.

The DTBM-SEGPHOS-or Ph-BPE-based CuH-protocol is not restricted to the synthesis of a range of structurally diverse optically active tertiary amines as described above. It has also been applicable to the preparation of various enantioenriched secondary (aryl)amines and amides and primary amines with high efficiency via structural alteration of the amine transfer agent and optimization of the reaction conditions (Figure 27). The use of the electron-rich ester *p*-NMe$_2$C$_6$H$_4$CO$_2$NHR^3 [168,169], 1,2-benzisoxazole [170] and substituted 2,1-benzisoxazoles [171] as modified electrophilic amine partners gives straightforward access to secondary amines, primary amines and secondary arylamines tethered to a benzylic alcohol respectively in moderate-to-good yields and high enantioinduction. For the reaction with benzisoxazole derivatives, a work-up is needed to liberate the amine functionality. Readily available 1,4,2-dioxazol-5-ones could also be employed as electrophilic amidating reagents to provide a direct access to amides from (hetereo)arylalkenes with high level of enantiopurity (Figure 27) [172–174].

Buchwald and Li 2015, 2018

Figure 27. Regio- and enantioselective biphosphine·CuH-catalyzed hydroamination of alkene derivatives and electrophilic amines. [a] all reactions run with Cu(OAc)$_2$, (*R*)- or (*S*)-**L$_3$**, HSiMe(OMe)$_2$ in THF unless otherwise stated. [b] PPh$_3$ (4.4–8.8 mol%). [c] after work-up with NH$_2$OH·HCl. [d] (*S,S*)-**L$_2$** (5.5 mol%), *t*-BuOH (2 equiv), cyclohexane. [e] after workup with NH$_4$F. [f] (*S,S*)-**L$_2$** (4.4 mol%), Ph$_2$SiH$_2$ (2 equiv), 1,4-dioxane/THF = 4:1. rt = room temperature, d.r = diasteromeric ratio, ee = enantiomeric excess.

This efficient umpolung amination strategy was further applied to the development of asymmetric *N*- and *C3*-selective alkylation methods of indoles (Figure 28) [175]. In these methods, indoles derivatives were used as electrophiles to circumvent the natural *C3*-alkylation of nucleophilic indoles. It was noted that the *N*-to *C3* regioselectivity of the CuH-catalyzed alkylation of indoles by styrene derivatives was ligand-controlled affording either enantioenriched *N*-alkylated indoles when (*R*)-DTBM-SEGPHOS was used as supporting ligand or *C3*-alkylated indoles when (*S,S*)-Ph-BPE was used (Figure 28) [170,176]. The employ of bulkier *N*-(2,4,6-trimethylbenzoyl)indole as electrophile is also important to slow down the reductive cleavage of N–O bond by the CuH species and allows the formation of the C–N bond. As a general trend, the DTBM-SEGPHOS-promoted *N*-alkylation reaction is more efficient than the Ph-BDE-promoted *C3*-alkylation in terms of yield, regioselectivity and enantioinduction as illustrated in Figure 28. Theoretical calculations rationalized the ligand-controlled regiodivergence observed in this transformation.

The broad generality, functional group tolerance, predictability and catalyst-control of this biphosphine-based CuH-methodology have paved the way for its successful integration into various auto-tandem catalytic process, providing access to numerous classes of amines, such as α-, γ-, or δ-chiral amines, β-amino acids or enamines from allylic derivatives [177], α, β-unsaturated carbonyl compounds [178,179], or alkynes [180,181], with high levels of regio-, stereo- and chemoselectivity. The synthetic utility of this methodology has also been demonstrated in late-stage preparation of numerous pharmaceutically relevant compounds [146,153,164,165,175].

Buchwald 2019
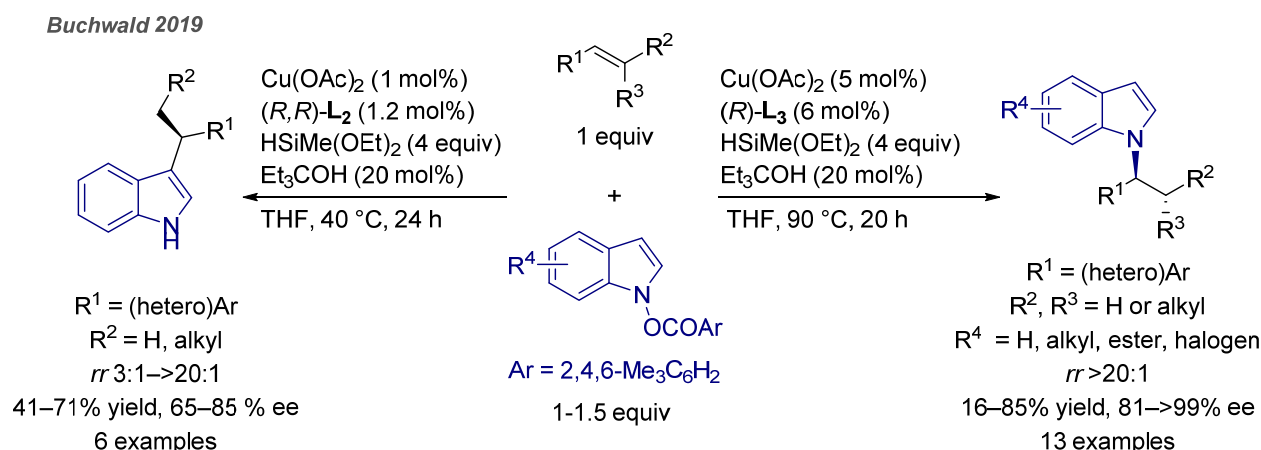
Figure 28. Ligand-controlled regiodivergent synthesis of *N*- and *C3*-alkylated enantioriched indoles by CuH-catalyzed hydroamination. *rr* = regioselectivity defined as ratio of *N*- and *C3*-isomer. ee = enantiomeric excess.
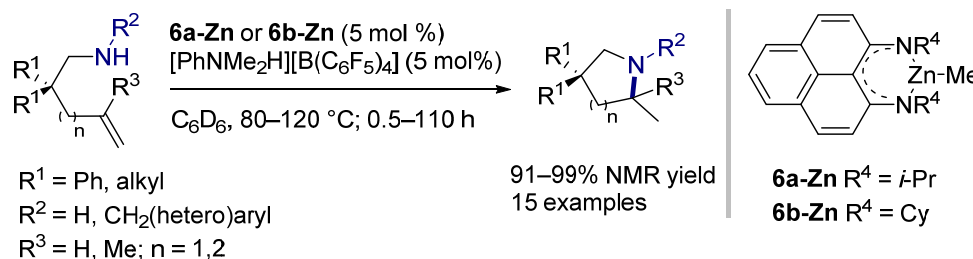
7. Zinc

7.1. Hydroalkoxylation

Very few zinc-based systems have been reported in the literature to catalyze the formation of C–O bond by hydroalkoxylation. Indeed, until 2019, to our knowledge, only Zn(OTf)$_2$ was reported by the group of Hii for the cyclohydroalkylation of γ–allenols. Whereas the more common 5-*exo*-trig selectivity was generally observed with various systems like AgOTf, Au and Pt catalysts for this transformation, in an interesting way, the unusual 6-*exo*-dig cyclization occurs mostly when the reaction is catalyzed by Zn(OTf)$_2$ [182]. In 2019, Chein et al. reported two efficient and mild catalytic Lewis acid-assisted Brønsted acid systems ZnI$_2$/TsOH and Zn(OTf)$_2$/TsOH for various intramolecular alkene hydrofunctionalization reactions, such as hydroalkoxylation, hydrocarboxylation, hydroamination, hydroamidation, hydroarylation and polyene cyclizations [183]. Although only three examples of formation of five- and six-membered cyclic ethers by hydroalkoxylation were reported, this protocol illustrates the potential of zinc-derived catalytic system to form C–O bond by this methodology.

7.2. Hydroamination

Various research groups have studied the potential of zinc in catalysis for hydroamination reactions [184,185]. The first examples of alkene cyclohydroamination catalyzed by zinc derivatives were reported by the Roesky group in 2005 using [*N*-isopropyl-2-(isopropylamino) troponiminato] methylzinc complex in the presence of [PhNMe$_2$H][B(C$_6$F$_5$)$_4$] as Brønsted acid co-catalyst [186]. Several modulations of the steric and electronic properties of the aminotroponimate skeleton were further attempted to improve the catalyst activity and stability [180,187,188]. Inspired by this original work, Mandal and co-workers reported well-defined alkyl zinc complexes **6a-Zn** and **6b-Zn** bearing a symmetrical *N*-isopropyl and *N*-cyclohexyl-substituted phenalenyl-based ligand respectively (Figure 29) [189,190]. These complexes, in the presence of [PhNMe$_2$H][B(C$_6$F$_5$)$_4$] co-catalyst, display similar catalytic activity to that of Roesky's [*N*-cyclohexyl-2-(cyclohexylamino)troponiminato] methylzinc complex for the conversion of functionalized primary and secondary aminoalkenes into five- and six-membered rings. As previously observed, the rate is improved in the presence of the Brønsted acid co-catalyst and altered by the nature of the ligand *N*-substituent.

Mandal 2012-2013

R^1 = Ph, alkyl
R^2 = H, CH$_2$(hetero)aryl
R^3 = H, Me; n = 1,2

91–99% NMR yield
15 examples

6a-Zn R^4 = *i*-Pr
6b-Zn R^4 = Cy

Figure 29. Intramolecular hydroamination of aminoalkenes catalyzed by phenalenyl-based organozinc complexes.

Li and co-workers described a very effective Zn(CF$_3$SO$_3$)$_2$-catalyzed domino intermolecular hydroamination-ring cleavage of 2,5-dihydrofuran with aniline derivatives (Figure 30) [191]. The homoallylic β-amino alcohols are obtained in moderate yields under mild reaction conditions. The authors propose that the Lewis acid Zn(CF$_3$SO$_3$)$_2$ induces the formation of anilinium triflate which can transfer a proton to 2,5-dihydrofuran leading to the formation of a carbocation. The carbocation is then attacked by the aniline derivative. At the same time, activated by the zinc triflate, the C–O bond of the alkene partner is cleaved by transfer of a triflate anion coming from the metal. Finally, formal elimination of triflic acid leads to the formation of the product terminal double bond.

Li 2013

R^1 = H, alkyl, 4-OMe, 4-OCF$_3$, 4-Cl
R^2 = Me, H

55–68% yield
10 examples
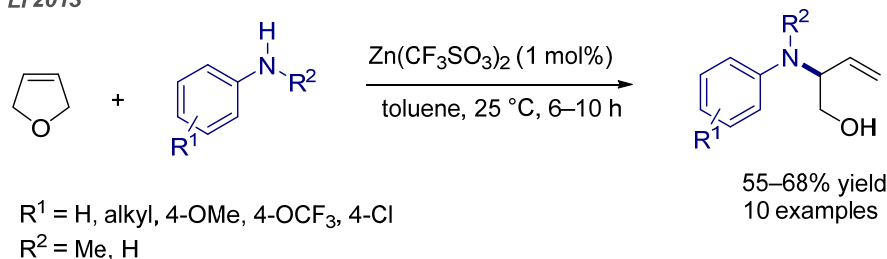
Figure 30. Zn(CF$_3$SO$_3$)$_2$-catalyzed hydroamination-ring cleavage of 2,5-dihydrofuran with aromatic amines.

More recently, the group of Nembenna prepared and fully characterized a zinc complex bearing bulky guanidinato and amido ligands [192]. This complex was very efficient for the intramolecular hydroamination for primary and secondary *N*-benzyl amines tethered to mono- and disubstituted alkenes. Reactions were carried out at 80 °C with 5 mol% of zinc guanidinate complex and gave the corresponding pyrrolidines and piperidines (14 examples) with almost total conversion in less than 4 h.

The first and sole demonstration of enantioselective Zn-promoted alkene hydroamination was done by the Hultzsch group in 2009 using a bis(organozinc) complex supported by a chiral L-proline modified diamidobinaphthyl ligand [193]. Although moderate enantioinduction were noticed for the cyclized products (<29% ee), the proof-of-principle was clearly established [194].

8. Conclusions

This review has put forward the most relevant advances of the last decade in the addition of E–H (E = O, N) σ–bond onto unactivated alkenes, 1,2- and 1,3-dienes promoted by manganese, iron, cobalt, nickel, copper and zinc catalysis. It is unquestionable that earth-abundant 3d metals have played a major role in the latest developments of metal-catalyzed alkene hydrofunctionalization as witnessed by the burgeoning activity highlighted herein. The inherent properties of these 3d elements have been a strong leverage for the emergence of alternative and complementary strategies that not only reckon on classical two-electron

reactivities but also on original one-electron reactivities. These novel strategies have led to some outstanding breakthroughs in terms of scope, control of (stereo)selectivities and applicability. The advent of the chiral biphosphine ligated copper-hydride chemistry with electrophilic amines has revolutionized the field and has brought the hydroamination methodology to a broad synthetic applicability that has never been reached by any other metal-catalyzed hydrofunctionalization process. The growing and fruitful exploitation of cobalt-hydride mediated HAT/radical polar crossover strategies for hydroamination and hydroalkoxylation, as well as iron-hydride mediated HAT for hydroamination, have also successfully reshaped the area via a controlled and metal-promoted radical-type reactivity. The former strategy has even tackled the challenging enantioselective alkene hydroalkoxylation, that has been poorly exploited by 3d late transition metal catalysis. However, these ground-breaking strategies are not without shortcomings as they usually require the need of a substoichiometric reducing agent and/or oxidant and so diverge from the original concept of step- and atom efficiency of direct alkene hydrofunctionalization. Nevertheless, significant advances in this direction have also been reached by iron, cobalt and copper catalysts via more classical activation pathways. Worth noting is also the rebirth of nickel catalysis that delivers efficient catalysts for the 1,3-diene hydrofunctionalization with high level of enantioinduction in hydroamination. Most of the 3d metal catalytic systems reported herein afford Markovnikov selectivity and only some of them display the opposite selectivity. This highlights the challenging issue of selectivity control as Markovnikov and anti-Markovnikov adducts are both compounds of interest. All these thriving advances have elegantly enriched the portfolio of strategies to construct C–O and C–N bond by earth-abundant 3d late transition metal-catalyzed hydrofunctionalization and will undoubtedly guide the development of fascinating synthetic chemistry in the near future.

Author Contributions: Writing—original draft preparation, L.R., D.C., A.S., H.Z., R.G., S.B., J.H.; writing—review and editing, J.H.; supervision, J.H. All authors have read and agreed to the published version of the manuscript.

References and Notes

1. Trowbridge, A.; Walton, S.M.; Gaunt, M.J. New Strategies for the Transition-Metal Catalyzed Synthesis of Aliphatic Amines. *Chem. Rev.* **2020**, *120*, 2613–2692. [CrossRef]
2. Elliot, M.C.; Williams, E. Saturated oxygen heterocycles. *J. Chem. Soc. Perkin Trans. 1* **2001**, *19*, 2303–2340. [CrossRef]
3. Müller, T.E.; Hultzsch, K.C.; Yus, M.; Foubelo, F.; Tada, M. Hydroamination: Direct Addition of Amines to Alkenes and Alkynes. *Chem. Rev.* **2008**, *108*, 3795–3892. [CrossRef] [PubMed]
4. Weiss, C.J.; Marks, T.J. Organo-f-element catalysts for efficient and highly selective hydroalkoxylation and hydrothiolation. *Dalton Trans.* **2010**, *39*, 6576–6588. [CrossRef]
5. Ananikov, V.P.; Tanaka, M. (Eds.) *Hydrofunctionalization*; Topics in Organometallic Chemistry; Springer: Berlin/Heidelberg, Germany, 2013; Volume 43, pp. 1–325.
6. Rodriguez-Ruiz, V.; Carlino, R.; Bezzenine-Lafollée, S.; Gil, R.; Prim, D.; Schulz, E.; Hannedouche, J. Recent Developments in Alkene Hydrofunctionalisation Promoted by Homogeneous Catalysts based on Earth Abundant Elements: Formation of C–N, C–O and C–P bond. *Dalton Trans.* **2015**, *44*, 12029–12059. [CrossRef]
7. Huang, L.; Arndt, M.; Gooßen, K.; Heydt, H.; Gooßen, L.J. Late Transition Metal-Catalyzed Hydroamination and Hydroamidation. *Chem. Rev.* **2015**, *115*, 2596–2697. [CrossRef] [PubMed]
8. Bezzenine-Lafollée, S.; Gil, R.; Prim, D.; Hannedouche, J. First-Row Late Transition Metals for Catalytic Alkene Hydrofunctionalisation: Recent Advances in C-N, C-O and C-P Bond Formation. *Molecules* **2017**, *22*, 1901. [CrossRef]
9. Xie, W.-B.; Li, Z. Asymmetric Synthesis of Ethers by Catalytic Alkene Hydroalkoxylation. *Synthesis* **2020**, *52*, 2127–2146.
10. Bernoud, E.; Lepori, C.; Mellah, M.; Schulz, E.; Hannedouche, J. Recent advances in metal free- and late transition metal-catalysed hydroamination of unactivated alkenes. *Catal. Sci. Technol.* **2015**, *5*, 2017–2037. [CrossRef]

11. Hannedouche, J.; Schulz, E. Asymmetric Hydroamination: A Survey of the Most Recent Developments. *Chem. Eur. J.* **2013**, *19*, 4972–4985. [CrossRef]

12. Nguyen, H.N.; Lee, H.; Audörsch, S.; Reznichenko, A.L.; Nawara-Hultzsch, A.J.; Schmidt, B.; Hultzsch, K.C. Asymmetric Intra- and Intermolecular Hydroamination Catalyzed by 3,3′-Bis(trisarylsilyl)- and 3,3′-Bis(arylalkylsilyl)-Substituted Binaphtholate Rare-Earth-Metal Complexes. *Organometallics* **2018**, *37*, 4358–4379. [CrossRef]

13. Zhou, Y.; Xu, X.; Sun, H.; Tao, G.; Chang, X.-Y.; Xing, X.; Chen, X. Development of highly efficient platinum catalysts for hydroalkoxylation and hydroamination of unactivated alkenes. *Nat. Commun.* **2021**, *12*, 1953–1963. [CrossRef]

14. Vanable, E.P.; Kennemur, J.L.; Joyce, L.A.; Ruck, R.T.; Schultz, D.M.; Hull, K.L. Rhodium-Catalyzed Asymmetric Hydroamination of Allyl Amines. *J. Am. Chem. Soc.* **2019**, *141*, 739–742. [CrossRef] [PubMed]

15. Schmidt, J.P.; Breit, B. Rhodium-Catalyzed Cyclization of Terminal and Internal Allenols: An Atom Economic and Highly Stereoselective Access towards Tetrahydropyrans. *Angew. Chem. Int. Ed.* **2020**, *59*, 23485–23490. [CrossRef] [PubMed]

16. Griffin, S.E.; Pacheco, J.; Schafer, L.L. Reversible C–N Bond Formation in the Zirconium-Catalyzed Intermolecular Hydroamination of 2-Vinylpyridine. *Organometallics* **2019**, *38*, 1011–1016. [CrossRef]

17. Chirik, P.; Morris, R. Getting Down to Earth: The Renaissance of Catalysis with Abundant Metals. *Acc. Chem. Res.* **2015**, *48*, 2495. [CrossRef] [PubMed]

18. Lard, S.W.; Schmidt, V.A. Intermolecular Radical Mediated Anti-Markovnikov Alkene Hydroamination Using N-Hydroxyphthalimide. *J. Am. Chem. Soc.* **2018**, *140*, 12318–12322. [CrossRef]

19. Chen, J.; Lu, Z. Recent Advances in Hydrometallation of Alkenes and Alkynes via the First Row Transition Metal Catalysis. *Chin. J. Chem.* **2018**, *36*, 1075–1109. [CrossRef]

20. Tsui, E.; Metrano, A.J.; Tsuchiya, Y.; Knowles, R.R. Catalytic Hydroetherification of Unactivated Alkenes Enabled by Proton-Coupled Electron Transfer. *Angew. Chem. Int. Ed.* **2020**, *59*, 11845–11849. [CrossRef]

21. Ganley, J.M.; Murray, P.R.D.; Knowles, R.R. Photocatalytic Generation of Aminium Radical Cations for C–N Bond Formation. *ACS Catal.* **2020**, *10*, 11712–11738. [CrossRef]

22. Roos, C.B.; Demaerel, J.; Graff, D.E.; Knowles, R.R. Enantioselective Hydroamination of Alkenes with Sulfonamides Enabled by Proton-Coupled Electron Transfer. *J. Am. Chem. Soc.* **2020**, *142*, 5974–5979. [CrossRef] [PubMed]

23. Francis, D.; Nelson, A.; Marsden, S.P. Synthesis of β-Diamine Building Blocks by Photocatalytic Hydroamination of Enecarbamates with Amines, Ammonia and N-H Heterocycles. *Chem. Eur. J.* **2020**, *26*, 14861–14865. [CrossRef] [PubMed]

24. Park, S.; Jeong, J.; Fujita, K.; Yamamoto, A.; Yoshida, H. Anti-Markovnikov Hydroamination of Alkenes with Aqueous Ammonia by Metal-Loaded Titanium Oxide Photocatalyst. *J. Am. Chem. Soc.* **2020**, *142*, 12708–12714. [CrossRef]

25. Nguyen, S.T.; Zhu, Q.; Knowles, R.R. PCET-Enabled Olefin Hydroamidation Reactions with *N*-Alkyl Amides. *ACS Catal.* **2019**, *9*, 4502–4507. [CrossRef] [PubMed]

26. Nguyen, L.Q.; Knowles, R.R. Catalytic C–N Bond-Forming Reactions Enabled by Proton-Coupled Electron Transfer Activation of Amide N–H Bonds. *ACS Catal.* **2016**, *6*, 2894–2903. [CrossRef]

27. Jiang, H.; Studer, A. Anti-Markovnikov Radical Hydro-and Deuteroamidation of UnactivatedAlkenes. *Chem. Eur. J.* **2019**, *25*, 7105–7109. [CrossRef]

28. Margrey, K.A.; Nicewicz, D.A. A General Approach to Catalytic Alkene Anti-Markovnikov Hydrofunctionalization Reactions via Acridinium Photoredox Catalysis. *Acc. Chem. Res.* **2016**, *49*, 1997–2006. [CrossRef]

29. Weiser, M.; Hermann, S.; Penner, A.; Wagenknecht, H.-A. Photocatalytic nucleophilic addition of alcohols to styrenes in Markovnikov and *anti*-Markovnikov orientation. *Beilstein J. Org. Chem.* **2015**, *11*, 568–575. [CrossRef]

30. Yang, Z.; Li, H.; Li, S.; Zhang, M.-T.; Luo, S. A chiral ion-pair photoredox organocatalyst: Enantioselective anti-Markovnikov hydroetherification of alkenols. *Org. Chem. Front.* **2017**, *4*, 1037–1041. [CrossRef]

31. Cheng, H.; Wang, X.; Chang, L.; Chen, Y.; Chu, L.; Zuo, Z. Bisphosphonium salt: An effective photocatalyst for the intramolecular hydroalkoxylation of olefins. *Sci. Bull.* **2019**, *64*, 1896–1901. [CrossRef]

32. Wang, H.; Man, Y.; Xiang, Y.; Wang, K.; Li, N.; Tang, B. Regioselective intramolecular Markovnikov and anti-Markovnikov hydrofunctionalization of alkenes via photoredox catalysis. *Chem. Commun.* **2019**, *55*, 11426–11429. [CrossRef] [PubMed]

33. Tsuji, N.; Kennemur, J.L.; Buyck, T.; Lee, S.; Prévost, S.; Kaib, P.S.J.; Bykov, D.; Farès, C.; List, B. Activation of olefins via asymmetric Brønsted acid catalysis. *Science* **2018**, *359*, 1501–1505. [CrossRef]

34. Yu, Z.-L.; Cheng, Y.-F.; Jiang, N.-C.; Wang, J.; Fan, L.-W.; Yuan, Y.; Li, Z.-L.; Gu, Q.-S.; Liu, X.-Y. Desymmetrization of unactivated bis-alkenes via chiral Brønsted acid-catalysed hydroamination. *Chem. Sci.* **2020**, *11*, 5987–5993. [CrossRef]

35. Guoa, J.; Teo, P. *Anti*-Markovnikov Oxidation and Hydration of Terminal Olefins. *Dalton Trans.* **2014**, *43*, 6952–6964. [CrossRef]

36. Bhunia, A.; Bergander, K.; Daniliuc, C.G.; Studer, A. Fe-Catalyzed Anaerobic Mukaiyama-Type Hydration of Alkenes using Nitroarenes. *Angew. Chem. Int. Ed.* **2021**, *60*, 8313–8320. [CrossRef] [PubMed]

37. Ferrand, L.; Tang, Y.; Aubert, C.; Fensterbank, L.; Mouriès-Mansuy, V.; Petit, M.; Amatore, M. Niobium-Catalyzed Intramolecular Addition of O-H and N-H Bonds to Alkenes: A Tool for Hydrofunctionalization. *Org. Lett.* **2017**, *19*, 2062–2065. [CrossRef]

38. Nagamoto, M.; Nishimura, T. Iridium-Catalyzed Asymmetric Cyclization of Alkenoic Acids Leading to γ-Lactones. *Chem. Commun.* **2015**, *51*, 13466–13469. [CrossRef]

39. Qi, C.; Yang, S.; Gandon, V.; Leboeuf, D. Calcium(II)- and Triflimide-Catalyzed Intramolecular Hydroacyloxylation of Unactivated Alkenes in Hexafluoroisopropanol. *Org. Lett.* **2019**, *21*, 7405–7409. [CrossRef]

40. Carney, J.R.; Dillon, B.R.; Thomas, S.P. Recent Advances of Manganese Catalysis for Organic Synthesis. *Eur. J. Org. Chem.* **2016**, *2016*, 3912–3929. [CrossRef]

41. Ji, Y.-X.; Li, J.; Li, C.-M.; Qu, S.; Zhang, B. Manganese-Catalyzed N–F Bond Activation for Hydroamination and Carboamination of Alkenes. *Org. Lett.* **2021**, *23*, 207–212. [CrossRef]

42. De Almeida, L.D.; Bourriquen, F.; Junge, K.; Beller, M. Catalytic Formal Hydroamination of Allylic Alcohols Using Manganese PNP-Pincer Complexes. *Adv. Synth. Catal.* **2021**, *363*. [CrossRef]

43. Cheng, W.-M.; Shang, R. Transition Metal-Catalyzed Organic Reactions under Visible Light: Recent Developments and Future Perspectives. *ACS Catal.* **2020**, *10*, 9170–9196. [CrossRef]

44. Greenhalgh, M.D.; Jones, A.S.; Thomas, S.P. Iron-catalysed Hydrofunctionalisation of Alkenes and Alkynes. *ChemCatChem* **2015**, *7*, 190–222. [CrossRef]

45. Alcaide, B.; Almendros, P.; Martínez del Campo, T.; Redondo, M.C.; Fernández, I. Striking Alkenol versus Allenol Reactivity: Metal-catalyzed Chemodifferentiating Oxycyclization of Enallenols. *Chem. Eur. J.* **2011**, *17*, 15005–15013. [CrossRef] [PubMed]

46. Alcaide, B.; Almendros, P.; Quirós, M.T. Accessing Skeletal Diversity under Iron Catalysis Using Substrate Control: Formation of Pyrroles versus Lactones. *Adv. Synth. Catal.* **2011**, *353*, 585–594. [CrossRef]

47. Komeyama, K.; Morimoto, T.; Nakayama, Y.; Takaki, K. Cationic iron-catalyzed Intramolecular Hydroalkoxylation of Unactivated Olefins. *Tetrahedron Lett.* **2007**, *48*, 3259–3261. [CrossRef]

48. Ke, F.; Li, Z.; Xiang, H.; Zhou, X. Catalytic Hydroalkoxylation of Alkenes by Iron(III) Catalyst. *Tetrahedron Lett.* **2011**, *52*, 318–320. [CrossRef]

49. Notar Francesco, I.; Cacciuttolo, B.; Pucheault, M.; Antoniotti, S. Simple metal salts supported on montmorillonite as recyclable catalysts for intramolecular hydroalkoxylation of double bonds in conventional and VOC-exempt solvents. *Green Chem.* **2015**, *17*, 837–841. [CrossRef]

50. Notar Francesco, I.; Cacciuttolo, B.; Pascu, O.; Aymonier, C.; Pucheault, M.; Antoniotti, S. Simple Salts of Abundant Metals (Fe, Bi, and Ti) Supported on Montmorillonite as Efficient and Recyclable Catalysts for Regioselective Intramolecular and Intermolecular Hydroalkoxylation Reactions of Double Bonds and Tandem Processes. *RCS Adv.* **2016**, *6*, 19807–19818. [CrossRef]

51. Jung, M.S.; Kim, W.S.; Shin, Y.H.; Jin, H.J.; Kim, Y.S.; Kang, E.J. Chemoselective Activities of Fe(III) Catalysts in the Hydrofunctionalization of Allenes. *Org. Lett.* **2012**, *14*, 6262–6265. [CrossRef]

52. Kim, J.H.; Kim, S.W.; Jung, M.S.; Ahn, K.-H.; Kang, E.J. Regioselectivities in Fe(III)-catalyzed Cycloisomerization Reactions of γ-Allenyl Alcohols. *Bull. Korean Chem. Soc.* **2015**, *36*, 2846–2850. [CrossRef]

53. El-Sepelgy, O.; Brzozowska, A.; Sklyaruk, J.; Jang, Y.K.; Zubar, V.; Rueping, M. Cooperative metal-ligand catalyzed intramolecular hydroamination and hydroalkoxylation of allenes using a stable iron catalyst. *Org. Lett.* **2018**, *20*, 696–699. [CrossRef] [PubMed]

54. Marcyk, P.T.; Cook, S.P. Iron-catalyzed hydroamination and hydroetherification of unactivated alkenes. *Org. Lett.* **2019**, *21*, 1547–1550. [CrossRef] [PubMed]

55. Komeyama, K.; Morimoto, T.; Takaki, K. A Simple and Efficient Iron-Catalyzed Intramolecular Hydroamination of Unactivated Olefins. *Angew. Chem. Int. Ed.* **2006**, *45*, 2938–2941. [CrossRef] [PubMed]

56. Michaux, J.; Terrasson, V.; Marque, S.; Wehbe, J.; Prim, D.; Campagne, J.-M. Intermolecular FeCl3-Catalyzed Hydroamination of Styrenes. *Eur. J. Org. Chem.* **2007**, *2007*, 2601–2603. [CrossRef]

57. Cheng, X.; Xia, Y.; Wei, H.; Xu, B.; Zhang, C.; Li, Y.; Qian, G.; Zhang, X.; Li, K.; Li, W. Lewis Acid Catalyzed Intermolecular Olefin Hydroamination: Scope, Limitation, and Mechanism. *Eur. J. Org. Chem.* **2008**, *2008*, 1929–1936. [CrossRef]

58. Dal Zotto, C.; Michaux, J.; Zarate-Ruiz, A.; Gayon, E.; Virieux, D.; Campagne, J.-M.; Terrasson, V.; Pieters, G.; Gaucher, A.; Prim, D. FeCl3-catalyzed addition of nitrogen and 1,3-dicarbonyl nucleophiles to olefins. *J. Organomet. Chem.* **2011**, *696*, 296–304. [CrossRef]

59. Shao, M.; Wu, Y.; Feng, Z.; Gu, X.; Wang, S. Synthesis of polysubstituted 1,2-dihydroquinolines and indoles via cascade reactions of arylamines and propargylic alcohols catalyzed by FeCl3·6H2O. *Org. Biomol. Chem.* **2016**, *14*, 2515–2521. [CrossRef]

60. Pérez, S.J.; Martin, A.P.; Cruz, D.A.; Ljpez-Soria, J.M.; Carballo, R.M.; Ramirez, M.A.; Fernandez, I.; Martin, V.S.; Padron, J.I. Enantiodivergent synthesis of (+)- and (−)-pyrrolidine 197B: Synthesis of trans-2,5-disubstituted pyrrolidines by intramolecular hydroamination. *Chem. Eur. J.* **2016**, *22*, 15529–15535. [CrossRef]

61. Marcyk, P.T.; Cook, S.P. Synthesis of Tetrahydroisoquinolines through an Iron-Catalyzed Cascade: Tandem Alcohol Substitution and Hydroamination. *Org. Lett.* **2019**, *21*, 6741–6744. [CrossRef]

62. Peng, Y.; Quin, C.; Chen, X.; Li, J.; Li, H.; Wang, W. Iron-catalyzed Anti-Markovnikov Hydroamination of Vinylpyridines. *Asian J. Org. Chem.* **2017**, *6*, 694–697. [CrossRef]

63. Xiao, E.; Wu, X.-T.; Ma, F.; Feng, X.; Chen, P.; Jiang, Y.-J. Fe(OTf)3- and γ-cycldextrin-catalyzed hydrooamination of alkenes with carbazoles. *Org. Lett.* **2021**, *23*, 449–453. [CrossRef] [PubMed]

64. Bernoud, E.; Oulié, P.; Guillot, R.; Mellah, M.; Hannedouche, J. Well-Defined Four-Coordinate Iron(II) Complexes For Intramolecular Hydroamination of Primary Aliphatic Alkenylamines. *Angew. Chem. Int. Ed.* **2014**, *53*, 4930–4934. [CrossRef]

65. Lepori, C.; Guillot, R.; Hannedouche, J. C_1-symmetric β-Diketiminatoiron(II) Complexes for Hydroamination of Primary Alkenylamines. *Adv. Synth. Catal.* **2019**, *361*, 714–719. [CrossRef]

66. Ma, W.; Zhang, X.; Fan, J.; Liu, Y.; Tang, W.; Xue, D.; Li, C.; Xiao, J.; Wang, C. Iron-Catalyzed Anti-Markovnikov Hydroamination and Hydroamidation of Allylic Alcohols. *J. Am. Chem. Soc.* **2019**, *141*, 13506–13515, For an elegant report that involves in situ generated activated alkene via a hydrogen-borrowing strategy. [CrossRef]

67. Huehls, C.B.; Lin, A.; Yang, J. Iron-Catalyzed Intermolecular Hydroamination of Styrenes. *Org. Lett.* **2014**, *16*, 3620–3623. [CrossRef]

68. Gui, J.; Pan, C.-M.; Jin, Y.; Qin, T.; Lo, J.C.; Lee, B.J.; Spergel, S.H.; Mertzman, M.E.; Pitts, W.J.; La Cruz, T.E.; et al. Practical olefin hydroamination with nitroarenes. *Science* **2015**, *348*, 886–891. [CrossRef]

69. Lo, J.C.; Gui, J.; Yabe, Y.; Pan, C.-M.; Baran, P.S. Functionalized Olefin Cross-Coupling to Construct Carbon–Carbon Bonds. *Nature* **2014**, *516*, 343–348. [CrossRef]

70. Kim, D.; Rahaman, S.M.W.; Mercado, B.Q.; Poli, R.; Holland, P.L. Roles of Iron Complexes in Catalytic Radical Alkene Cross-Coupling: A Computational and Mechanistic Study. *J. Am. Chem. Soc.* **2019**, *141*, 7473, An unobserved iron(III)-H species could be speculated as the species [Fe^n]-H. [CrossRef]

71. Villa, M.; von Wangelin, A.J. Hydroaminations of Alkenes: A Radical, Revised, and Expanded Version. *Angew. Chem. Int. Ed.* **2015**, *54*, 11906–11908. [CrossRef]

72. Obradors, C.; Martinez, R.M.; Shenvi, R.A. Ph(i-PrO)SiH$_2$: An Exceptional Reductant for Metal-Catalyzed Hydrogen Atom Transfers. *J. Am. Chem. Soc.* **2016**, *138*, 4962–4971. [CrossRef] [PubMed]

73. Zhu, K.; Shaver, M.P.; Thomas, S.P. Amine-bis(phenolate) Iron(III)-Catalyzed Formal Hydroamination of Olefins. *Chem. Asian J.* **2016**, *11*, 977–980. [CrossRef] [PubMed]

74. Zhu, K.; Shaver, M.P.; Thomas, S.P. Chemoselective Nitro Reduction and Hydroamination Using a Single Iron Catalyst. *Chem. Sci.* **2016**, *7*, 3031–3035. [CrossRef] [PubMed]

75. Song, H.; Yang, Z.; Tung, C.-H.; Wang, W. Iron-catalyzed reductive coupling of nitroarenes with olefins: Intermediate of iron–nitroso complex. *ACS Catal.* **2020**, *10*, 276–281. [CrossRef]

76. Crossley, S.W.M.; Martinez, R.M.; Obradors, C.; Shenvi, R.A. Mn, Fe, and Co-catalyzed radical hydrofunctionalizations of olefins. *Chem. Rev.* **2016**, *116*, 8912–9000. [CrossRef]

77. Isayama, S.; Mukaiyama, T. A New Method for Preparation of Alcohols from Olefins with Molecular Oxygen and Phenylsilane by the Use of Bis(acetylacetonato)cobalt(II). *Chem. Lett.* **1989**, *18*, 1071–1074. [CrossRef]

78. Waser, J.; Carreira, E.M. Convenient Synthesis of Alkylhydrazides by the Cobalt-Catalyzed Hydrohydrazination Reaction of Olefins and Azodicarboxylates. *J. Am. Chem. Soc.* **2004**, *126*, 5676–5677. [CrossRef]

79. Waser, J.; Nambu, H.; Carreira, E.M. Cobalt-Catalyzed Hydroazidation of Olefins: Convenient Access to Alkyl Azides. *J. Am. Chem. Soc.* **2005**, *127*, 8294–8295. [CrossRef]

80. Gaspar, B.; Carreira, E.M. Mild Cobalt-Catalyzed Hydrocyanation of Olefins with Tosyl Cyanide. *Angew. Chem. Int. Ed.* **2007**, *46*, 4519–4522. [CrossRef] [PubMed]

81. Gaspar, B.; Carreira, E.M. Catalytic Hydrochlorination of Unactivated Olefins with *para*-Toluenesulfonyl Chloride. *Angew. Chem. Int. Ed.* **2008**, *47*, 5758–5760. [CrossRef]

82. Shigehisa, H.; Aoki, T.; Yamaguchi, S.; Shimizu, N.; Hiroya, K. Hydroalkoxylation of Unactivated Olefins with Carbon Radicals and Carbocation Species as Key Intermediates. *J. Am. Chem. Soc.* **2013**, *135*, 10306–10309. [CrossRef]

83. Shigehisa, H.; Kikuchi, H.; Hiroya, K. Markovnikov-Selective Addition of Fluorous Solvents to Unactivated Olefins Using a Co Catalyst. *Chem. Pharm. Bull.* **2016**, *64*, 371–374. [CrossRef] [PubMed]

84. Shepard, S.M.; Diaconescu, P.L. Redox-switchable Hydroelementation of a Cobalt Complex Supported by a Ferrocene-based Ligand. *Organometallics* **2016**, *35*, 2446–2453. [CrossRef]

85. Shigehisa, H.; Hayashi, M.; Ohkawa, H.; Suzuki, T.; Okayasu, H.; Mukai, M.; Yamazaki, A.; Kawai, R.; Kikuchi, H.; Satoh, Y.; et al. Catalytic Synthesis of Saturated Oxygen Heterocycles by Hydrofunctionalization of Unactivated Olefins: Unprotected and Protected Strategies. *J. Am. Chem. Soc.* **2016**, *138*, 10597–10604. [CrossRef] [PubMed]

86. Nagai, T.; Mimata, N.; Terada, Y.; Sebe, C.; Shigehisa, H. Catalytic Dealkylative Synthesis of Cyclic Carbamates and Ureas via Hydrogen Atom Transfer and Radical-Polar Crossover. *Org. Lett.* **2020**, *22*, 5522–5527. [CrossRef] [PubMed]

87. Touney, E.E.; Foy, N.J.; Pronin, S.V. Catalytic Radical–Polar Crossover Reactions of Allylic Alcohols. *J. Am. Chem. Soc.* **2018**, *140*, 16982–16987. [CrossRef] [PubMed]

88. Discolo, C.A.; Touney, E.E.; Pronin, S.V. Catalytic Asymmetric Radical-Polar Crossover Hydroalkoxylation. *J. Am. Chem. Soc.* **2019**, *141*, 17527–17532. [CrossRef]

89. Ebisawa, K.; Izumi, K.; Ooka, Y.; Kato, H.; Kanazawa, S.; Komatsu, S.; Nishi, E.; Shigehisa, H. Catalyst- and silane- controlled enantioselective hydrofunctionalization of alkenes by TM-HAT and RPC mechanism. *J. Am. Chem. Soc.* **2020**, *142*, 13481–13490. [CrossRef]

90. Shigehisa, H.; Koseki, N.; Shimizu, N.; Fujisawa, M.; Niitsu, M.; Hiroya, K. Catalytic Hydroamination of Unactivated Olefins Using a Co Catalyst for Complex Molecule Synthesis. *J. Am. Chem. Soc.* **2014**, *136*, 13534–13537. [CrossRef]

91. Ohuchi, S.; Koyama, H.; Shigehisa, H. Catalytic Synthesis of Cyclic Guanidines via Hydrogen Atom Transfer and Radical-Polar Crossover. *ACS Catal.* **2021**, *11*, 900–906. [CrossRef]

92. Yahata, K.; Kaneko, Y.; Akai, S. Cobalt-Catalyzed Intermolecular Markovnikov Hydroamination of Nonactivated Olefins: N^2-Selective Alkylation of Benzotriazole. *Org. Lett.* **2020**, *22*, 598–603. [CrossRef]

93. Yahata, K.; Kaneko, Y.; Akai, S. Cobalt-Catalyzed Hydroamination of Alkenes with 5-Substituted Tetrazoles: Facile Access to 2,5-Disubstituted Tetrazoles and Asymmetric Intermolecular Hydroaminations. *Chem. Pharm. Bull.* **2020**, *68*, 332–335. [CrossRef] [PubMed]

94.   Shen, X.; Chen, X.; Chen, J.; Sun, Y.; Cheng, Z.; Lu, Z. Ligand-promoted cobalt-catalyzed radical hydroamination of alkenes. *Nat. Commun.* **2020**, *11*, 783–790. [CrossRef]

95.   Chen, J.; Shen, X.; Lu, Z. Cobalt-Catalyzed Markovnikov Selective Sequential Hydrogenation/Hydrohydrazidation of Aliphatic Terminal Alkynes. *J. Am. Chem. Soc.* **2020**, *142*, 14455–14460. [CrossRef] [PubMed]

96.   Sun, H.-L.; Yang, F.; Ye, W.-T.; Wang, J.-J.; Zhu, R. Dual Cobalt and Photoredox Catalysis Enabled Intermolecular Oxidative Hydrofunctionalization. *ACS Catal.* **2020**, *10*, 4983–4989. [CrossRef]

97.   Zhou, X.-L.; Yang, F.; Sun, H.-L.; Yin, Y.-N.; Ye, W.-T.; Zhu, R. Cobalt-Catalyzed Intermolecular Hydrofunctionalization of Alkenes: Evidence for a Bimetallic Pathway. *J. Am. Chem. Soc.* **2019**, *141*, 7250–7255, For previous work of the group that uses hypervalent iodine(III) as two-electron oxidant for intermolecular alkene hydrofunctionalization with O- and N-based nucleophiles featuring a unique bimetallic-mediated coupling between organocobalt(III) and Co(III)-nucleophile. [CrossRef] [PubMed]

98.   Lepori, C.; Gomez-Orellana, P.; Ouharzoune, A.; Guillot, R.; Lledos, A.; Ujaque, G.; Hannedouche, J. Well-Defined β-Diketiminatocobalt(II) Complexes for Alkene Cyclohydroamination of Primary Amines. *ACS Catal.* **2018**, *8*, 4446–4451. [CrossRef]

99.   Schroeter, F.; Lerch, S.; Kaliner, M.; Strassner, T. Cobalt-Catalyzed Hydroarylations and Hydroaminations of Alkenes in Tunable Aryl Alkyl Ionic Liquids. *Org. Lett.* **2018**, *20*, 6215–6219, For a report on the use of cobalt salts in ionic liquids. [CrossRef]

100. Bigot, S.; El Alami, M.S.I.; Mifleur, A.; Castanet, Y.; Suisse, I.; Mortreux, A.; Sauthier, M. Nickel-catalysed Hydroalkoxylation Reaction of 1,3-Butadiene: Ligand Controlled Selectivity for the Efficient and Atom-economical Synthesis of Alkylbutenyl Ethers. *Chem. Eur. J.* **2013**, *19*, 9785–9788. [CrossRef]

101. Mifleur, A.; Ledru, H.; Lopes, A.; Suisse, I.; Mortreux, A.; Sauthier, M. Synthesis of Short-chain Alkenyl Ethers from Primary and Biosourced Alcohols via the Nickel-catalyzed Hydroalkoxylation Reaction of Butadiene and Derivatives. *Adv. Synth. Catal.* **2016**, *358*, 110–121. [CrossRef]

102. Mifleur, A.; Merel, D.; Mortreux, D.; Suisse, I.; Capet, F.; Trivelli, X.; Sauthier, M.; Macgregor, S.A. Deciphering the mechanism of the nickel-catalyzed hydroalkoxylation reaction: A combined experimental and computational study. *ACS Catal.* **2017**, *7*, 6915–6923. [CrossRef]

103. Mifleur, A.; Mortreux, A.; Suisse, I.; Sauthier, M. Synthesis of C4 Chain Glyceryl Ethers via Nickel-catalyzed Butadiene Hydroalkoxylation Reaction. *J. Mol. Catal. A Chem.* **2017**, *427*, 25–30. [CrossRef]

104. Mifleur, A.; Suisse, I.; Mortreux, A.; Sauthier, M. Enantioselective Nickel Catalyzed Butadiene Hydroalkoxylation with Ethanol: From Experimental Results to Kinetics Parameters. *Catal. Lett.* **2021**, *151*, 27–35, For a preliminary study towards an enantioselective Nickel-catalyzed butadiene hydroalkoxylation with ethanol. [CrossRef]

105. Tran, G.; Mazet, C. Ni-Catalyzed Regioselective Hydroalkoxylation of Branched 1,3-Dienes. *Org. Lett.* **2019**, *21*, 9124–9127. [CrossRef] [PubMed]

106. Baker, R.; Cook, A.H.; Halliday, D.E.; Smith, T.N. Reaction of amines with 1,3-dienes catalysed by nickel complexes. *J. Chem. Soc. Perkin Trans. 2* **1974**, 1511–1517. [CrossRef]

107. Baker, R.; Onions, A.; Popplestone, R.J.; Smith, T.N. Reactions of amines and active methylene compounds with buta-1,3-diene and isoprene: Catalysis by nickel, cobalt, rhodium, and iridium complexes. *J. Chem. Soc. Perkin Trans. 2* **1975**, 1133–1138. [CrossRef]

108. Pawlas, J.; Nakao, Y.; Kawatsura, M.; Hartwig, J.F. A General Nickel-Catalyzed Hydroamination of 1,3-Dienes by Alkylamines: Catalyst Selection, Scope, and Mechanism. *J. Am. Chem. Soc.* **2002**, *124*, 3369–3679. [CrossRef]

109. Tran, G.; Shao, W.; Mazet, C. Ni-Catalyzed Enantioselective Intermolecular Hydroamination of Branched 1,3-Dienes Using Primary Aliphatic Amines. *J. Am. Chem. Soc.* **2019**, *141*, 14814–14822. [CrossRef]

110. Long, J.; Wang, P.; Wang, W.; Li, Y.; Yin, G. Nickel/Brønsted Acid-Catalyzed Chemo- and Enantioselective Intermolecular Hydroamination of Conjugated Dienes. *iScience* **2019**, *22*, 369–379. [CrossRef]

111. Tafazolian, H.; Schmidt, J.A.R. Cationic [(Iminophosphine)nickel(allyl)]+ Complexes as the First Example of Nickel Catalysts for Direct Hydroamination of Allenes. *Chem. Eur. J.* **2017**, *23*, 1507–1511. [CrossRef]

112. Xiao, J.; He, Y.; Ye, F.; Zhu, S. Remote sp3 C–H Amination of Alkenes with Nitroarenes. *Chem* **2018**, *4*, 1645–1657. [CrossRef]

113. Jeon, J.; Lee, C.; Seo, H.; Hong, S. NiH-Catalyzed Proximal-Selective Hydroamination of Unactivated Alkenes. *J. Am. Chem. Soc.* **2020**, *142*, 20470–20480. [CrossRef] [PubMed]

114. Taylor, J.G.; Whittall, N.; Hii, K.K.M. Copper(II)-catalysed Addition of O-H Bonds to Norbornene. *Chem. Commun.* **2005**, 5103–5105. [CrossRef] [PubMed]

115. Adrio, L.A.; Hii, K.K.M. A Recyclable Copper(II) Catalyst for the Annulation of Phenols with 1,3-Dienes. *Chem. Commun.* **2008**, 2325–2327. [CrossRef] [PubMed]

116. Tschan, M.J.-L.; Thomas, C.M.; Strub, H.; Carpentier, J.-F. Copper(II) Triflate as a Source of Triflic Acid: Effective, Green Catalysis of Hydroalkoxylation Reactions. *Adv. Synth. Catal.* **2009**, *351*, 2496–2504. [CrossRef]

117. Murayama, H.; Nagao, K.; Ohmiya, H.; Sawamura, M. Copper(I)-catalyzed Intramolecular Hydroalkoxylation of Unactivated Alkenes. *Org. Lett.* **2015**, *17*, 2039–2041. [CrossRef]

118. Miller, Y.; Miao, L.; Hosseini, A.S.; Chemler, S.R. Copper-Catalyzed Enantioselective Intramolecular Alkene Amination/Intermolecular Heck-Type Coupling Cascade. *J. Am. Chem. Soc.* **2012**, *134*, 12149–12156. [CrossRef]

119. Bovino, M.T.; Liwosz, T.W.; Kendel, N.E.; Miller, Y.; Tyminska, N.; Zurek, E.; Chemler, S.R. Enantioselective Copper-Catalyzed Carboetherification of Unactivated Alkenes. *Angew. Chem. Int. Ed.* **2014**, *53*, 6383–6387. [CrossRef]

120. Chen, D.; Chemler, S.R. Synthesis of Phthalans Via Copper-Catalyzed Enantioselective Cyclization/Carboetherification of 2-Vinylbenzyl Alcohols. *Org. Lett.* **2018**, *20*, 6453–6456. [CrossRef]

121. Karyakarte, S.D.; Um, C.; Berhane, I.A.; Chemler, S.R. Synthesis of Spirocyclic Ethers by Enantioselective Copper-Catalyzed Carboetherification of Alkenols. *Angew. Chem. Int. Ed.* **2018**, *57*, 12921–12924. [CrossRef]

122. Chen, D.; Berhane, I.A.; Chemler, S.R. Copper-Catalyzed Enantioselective Hydroalkoxylation of Alkenols for the Synthesis of Cyclic Ethers. *Org. Lett.* **2020**, *22*, 7409–7414. [CrossRef] [PubMed]

123. Taylor, J.G.; Whittall, N.; Hii, K.K. Copper-Catalyzed Intermolecular Hydroamination of Alkenes. *Org. Lett.* **2006**, *8*, 3561–3564. [CrossRef]

124. Turnpenny, B.W.; Hyman, K.L.; Chemler, S.R. Chiral Indoline Synthesis via Enantioselective Intramolecular Copper-Catalyzed Alkene Hydroamination. *Organometallics* **2012**, *31*, 7819–7822. [CrossRef] [PubMed]

125. Michon, C.; Medina, F.; Capet, F.; Roussel, P.; Agbossou-Niedercorn, F. Inter- and Intramolecular Hydroamination of Unactivated Alkenes Catalysed by a Combination of Copper and Silver Salts: The Unveiling of a Brønstedt Acid Catalysis. *Adv. Synth. Catal.* **2010**, *35*, 3293–3305. [CrossRef]

126. Ohmiya, H.; Moriya, T.; Sawamura, M. Cu(I)-Catalyzed Intramolecular Hydroamination of Unactivated Alkenes Bearing a Primary or Secondary Amino Group in Alcoholic Solvents. *Org. Lett.* **2009**, *11*, 2145–2147. [CrossRef] [PubMed]

127. Ohmiya, H.; Yoshida, M.; Sawamura, M. Protecting-Group-Free Route to Hydroxylated Pyrrolidine and Piperidine Derivatives through Cu(I)-Catalyzed Intramolecular Hydroamination of Alkenes. *Synlett* **2010**, *2010*, 2136–2140.

128. Blieck, R.; Bahri, J.; Taillefer, M.; Monnier, F. Copper-Catalyzed Hydroamination of Terminal Allenes. *Org. Lett.* **2016**, *18*, 1482–1485. [CrossRef]

129. Tsuhako, A.; Oikawa, D.; Sakai, K.; Okamoto, S. Copper-catalyzed intramolecular hydroamination of allenylamines to 3-pyrrolines or 2-alkenylpyrrolidines. *Tetrahedron Lett.* **2008**, *49*, 6529–6532. [CrossRef]

130. Blieck, R.; Taillefer, M.; Monnier, F. Metal-Catalyzed Intermolecular Hydrofunctionalization of Allenes: Easy Access to Allylic Structures via the Selective Formation of C–N, C–C, and C–O Bonds. *Chem. Rev.* **2020**, *24*, 13545–13598. [CrossRef]

131. Xiong, Y.; Zhang, G. Visible-Light-Induced Copper-Catalyzed Intermolecular Markovnikov Hydroamination of Alkenes. *Org. Lett.* **2019**, *21*, 7873–7877, For an interesting a photo-induced Cu(NCMe)4(PF6)-catalyzed hydroamination of styrenes with aromatic amines. [CrossRef]

132. Perego, L.A.; Blieck, R.; Groué, A.; Monnier, F.; Taillefer, M.; Ciofini, I.; Grimaud, L. Copper-Catalyzed Hydroamination of Allenes: From Mechanistic Understanding to Methodology Development. *ACS Catal.* **2017**, *7*, 4253–4264. [CrossRef]

133. Perego, L.A.; Blieck, R.; Michel, J.; Ciofini, I.; Grimaud, L.; Taillefer, M.; Monnier, F. Copper-Catalyzed Hydroamination of N-Allenylazoles: Access to Amino-Substituted N-Vinylazoles. *Adv. Synth. Catal.* **2017**, *359*, 4388–4392. [CrossRef]

134. Blieck, R.; Perego, L.A.; Ciofini, I.; Grimaud, L.; Taillefer, M.; Monnier, F. Copper-Catalysed Hydroamination of N-Allenylsulfonamides: The Key Role of Ancillary Coordinating Groups. *Synthesis* **2019**, *51*, 1225–1234. [CrossRef]

135. Philippova, A.N.; Vorobyeva, D.V.; Monnier, F.; Osipov, S.N. Synthesis of α-CF$_3$-substituted E-dehydroornithine derivatives via copper(I)-catalyzed hydroamination of allenes. *Org. Biomol. Chem.* **2020**, *18*, 3274–3280. [CrossRef] [PubMed]

136. Miki, Y.; Hirano, K.; Satoh, T.; Miura, M. Copper-Catalyzed Intermolecular Regioselective Hydroamination of Styrenes with Polymethylhydrosiloxane and Hydroxylamines. *Angew. Chem. Int. Ed.* **2013**, *52*, 10830–10834. [CrossRef]

137. Zhu, S.; Niljianskul, N.; Buchwald, S.L. Enantio- and Regioselective CuH-Catalyzed Hydroamination of Alkenes. *J. Am. Chem. Soc.* **2013**, *135*, 15746–15749. [CrossRef] [PubMed]

138. Pirnot, M.T.; Wang, Y.-M.; Buchwald, S.L. Copper Hydride Catalyzed Hydroamination of Alkenes and Alkynes. *Angew. Chem. Int. Ed.* **2016**, *55*, 48–57. [CrossRef]

139. Liu, Y.R.; Buchwald, S.L. CuH-Catalyzed Olefin Functionalization: From Hydroamination to Carbonyl Addition. *Acc. Chem. Res.* **2020**, *53*, 1229–1243. [CrossRef] [PubMed]

140. Deutsch, C.; Krause, N.; Lipshutz, B.H. CuH-Catalyzed Reactions. *Chem. Rev.* **2008**, *108*, 2916–2927. [CrossRef] [PubMed]

141. Jordan, A.J.; Lalic, G.; Sadighi, J.P. Coinage Metal Hydrides: Synthesis, Characterization, and Reactivity. *Chem. Rev.* **2016**, *116*, 8318–8372. [CrossRef] [PubMed]

142. Corpet, M.; Gosmini, C. Recent Advances in Electrophilic Amination Reactions. *Synlett* **2014**, *46*, 2258–2271.

143. Miki, Y.; Hirano, K.; Satoh, T.; Miura, M. Copper-Catalyzed Enantioselective Formal Hydroamination of Oxa- and Azabicyclic Alkenes with Hydrosilanes and Hydroxylamines. *Org. Lett.* **2014**, *16*, 1498–1501. [CrossRef]

144. Bandar, J.S.; Pirnot, M.T.; Buchwald, S.L. Mechanistic Studies Lead to Dramatically Improved Reaction Conditions for the Cu-Catalyzed Asymmetric Hydroamination of Olefins. *J. Am. Chem. Soc.* **2015**, *137*, 14812–14818. [CrossRef]

145. Tobisch, S. CuH-Catalysed Hydroamination of Styrene with Hydroxylamine Esters: A Coupled Cluster Scrutiny of Mechanistic Pathways. *Chem. Eur. J.* **2016**, *22*, 8290–8300. [CrossRef] [PubMed]

146. Lu, G.; Liu, R.Y.; Yang, Y.; Fang, C.; Lambrecht, D.S.; Buchwald, S.L.; Liu, P. Ligand–Substrate Dispersion Facilitates the Copper-Catalyzed Hydroamination of Unactivated Olefins. *J. Am. Chem. Soc.* **2017**, *139*, 16548–16555. [CrossRef] [PubMed]

147. Thomas, A.A.; Speck, K.; Kevlishvili, I.; Lu, Z.; Liu, P.; Buchwald, S.L. Mechanistically Guided Design of Ligands That Significantly Improve the Efficiency of CuH-Catalyzed Hydroamination Reactions. *J. Am. Chem. Soc.* **2018**, *140*, 13976–13984. [CrossRef]

148. Niljianskul, N.; Zhu, S.; Buchwald, S.L. Enantioselective Synthesis of α-Aminosilanes by Copper-Catalyzed Hydroamination of Vinylsilanes. *Angew. Chem. Int. Ed.* **2015**, *54*, 1638–1641. [CrossRef]

149. Zhu, S.; Buchwald, S.L. Enantioselective CuH-Catalyzed Anti-Markovnikov Hydroamination of 1,1-Disubstituted Alkenes. *J. Am. Chem. Soc.* **2014**, *136*, 15913–15916. [CrossRef]

150. Yang, Y.; Shi, S.-L.; Niu, D.; Liu, P.; Buchwald, S.L. Catalytic Asymmetric Hydroamination of Unactivated Internal Olefins to Aliphatic Amines. *Science* **2015**, *349*, 62–66. [CrossRef]

151. Xi, Y.; Butcher, T.W.; Zhang, J.; Hartwig, J.F. Regioselective, Asymmetric Formal Hydroamination of Unactivated Internal Alkenes. *Angew. Chem. Int. Ed.* **2016**, *55*, 776–780. [CrossRef]

152. Nishikawa, D.; Hirano, K.; Miura, M. Asymmetric Synthesis of α-Aminoboronic Acid Derivatives by Copper-Catalyzed Enantioselective Hydroamination. *J. Am. Chem. Soc.* **2015**, *137*, 15620–15623. [CrossRef] [PubMed]

153. Takata, T.; Nishikawa, D.; Hirano, K.; Miura, M. Synthesis of a-Aminophosphines by Copper-Catalyzed Regioselective Hydroamination of Vinylphosphines. *Chem. Eur. J.* **2018**, *24*, 10975–10978. [CrossRef] [PubMed]

154. Takata, T.; Hirano, K.; Miura, M. Synthesis of α-Trifluoromethylamines by Cu-Catalyzed Regio- and Enantioselective Hydroamination of 1-Trifluoromethylalkenes. *Org. Lett.* **2019**, *21*, 4284–4288. [CrossRef] [PubMed]

155. Yu, L.; Somfai, P. Regio- and Enantioselective Formal Hydroamination of Enamines for the Synthesis of 1,2-Diamines. *Angew. Chem. Int. Ed.* **2019**, *58*, 8551–8555. [CrossRef]

156. Ichikawa, S.; Dai, X.-J.; Buchwald, S.L. Regio- and Enantioselective Synthesis of 1,2-Diamine Derivatives by Copper-Catalyzed Hydroamination. *Org. Lett.* **2019**, *21*, 4370–4373. [CrossRef] [PubMed]

157. Ichikawa, S.; Buchwald, S.L. Asymmetric Synthesis of γ-Amino Alcohols by Copper-Catalyzed Hydroamination. *Org. Lett.* **2019**, *21*, 8736–8739. [CrossRef] [PubMed]

158. Ichikawa, S.; Zhu, S.; Buchwald, S.L. A Modified System for the Synthesis of Enantioenriched N-Arylamines through Copper-Catalyzed Hydroamination. *Angew. Chem. Int. Ed.* **2018**, *55*, 8714–8718. [CrossRef]

159. Wang, H.; Yang, J.C.; Buchwald, S.L. CuH-Catalyzed Regioselective Intramolecular Hydroamination for the Synthesis of Alkyl-Substituted Chiral Aziridines. *J. Am. Chem. Soc.* **2017**, *139*, 8428–8431. [CrossRef]

160. Dai, X.-J.; Engl, O.D.; León, T.; Buchwald, S.L. Catalytic Asymmetric Synthesis of a-Arylpyrrolidines and Benzo-fused Nitrogen Heterocycles. *Angew. Chem. Int. Ed.* **2019**, *58*, 3407–3411. [CrossRef]

161. It was noted that both (*E*)- and (*Z*)-vinylsilanes afford the same enantiomer, but (*E*)-isomers are obtained with faster reaction rates and with higher ee values than (*Z*)-isomers, see ref. [148].

162. For an isolated example of hydroamination of a (*Z*)-1,2-dialkylsubstituted alkene in low yield and with low ee, see ref. [151].

163. Yang, Q.; Li, S.; Wang, J. Asymmetric Synthesis of Chiral Chromanes by Copper-Catalyzed Hydroamination of 2H-Chromenes. *ChemCatChem* **2020**, *12*, 3202–3206. [CrossRef]

164. Xu-Xu, Q.-F.; Zhang, X.; You, S.-L. Enantioselective Synthesis of 4-Aminotetrahydroquinolines via 1,2-Reductive Dearomatization of Quinolines and Copper(I) Hydride-Catalyzed Asymmetric Hydroamination. *Org. Lett.* **2019**, *21*, 5357–5362. [CrossRef] [PubMed]

165. Xu-Xu, Q.-F.; Liu, Q.-Q.; Zhang, X.; You, S.-L. Copper-Catalyzed Ring Opening of Benzofurans and an Enantioselective Hydroamination Cascade. *Angew. Chem. Int. Ed.* **2018**, *57*, 15204–15208. [CrossRef]

166. Nishikawa, D.; Sakae, R.; Miki, Y.; Hirano, K.; Miura, M.J. Copper-Catalyzed Regioselective Ring-Opening Hydroamination of Methylenecyclopropanes. *Org. Chem.* **2016**, *81*, 12128–12134. [CrossRef] [PubMed]

167. Feng, S.; Hao, H.; Liu, P.; Buchwald, S.L. Diastereo- and Enantioselective CuH-Catalyzed Hydroamination of Strained Trisubstituted Alkenes. *ACS Catal.* **2020**, *10*, 282–291. [CrossRef]

168. Niu, D.; Buchwald, S.L. Design of Modified Amine Transfer Reagents Allows the Synthesis of α-Chiral Secondary Amines via CuH-Catalyzed Hydroamination. *J. Am. Chem. Soc.* **2015**, *137*, 9716–9721. [CrossRef] [PubMed]

169. Romano, C.; Fiorito, D.; Mazet, C. Remote Functionalization of α,β-Unsaturated Carbonyls by Multimetallic Sequential Catalysis. *J. Am. Chem. Soc.* **2019**, *141*, 16983–16990, For an elegant integration of the methodology in [Pd/Cu]-catalyzed deconjugation isomerization/α-hydroamination sequence. [CrossRef] [PubMed]

170. Guo, S.; Yang, J.C.; Buchwald, S.L. Practical Electrophilic Nitrogen Source for the Synthesis of Chiral Primary Amines by Copper-Catalyzed Hydroamination. *J. Am. Chem. Soc.* **2018**, *140*, 15976–15984. [CrossRef] [PubMed]

171. Xie, F.; Shen, B.; Li, X. Enantioselective Copper-Catalyzed Hydroamination of Vinylarenes with Anthranils. *Org. Lett.* **2018**, *20*, 7154–7157. [CrossRef] [PubMed]

172. Zhou, Y.; Engl, O.D.; Bandar, J.S.; Chant, E.D.; Buchwald, S.L. CuH-Catalyzed Asymmetric Hydroamidation of Vinylarenes. *Angew. Chem. Int. Ed.* **2018**, *57*, 6672–6675. [CrossRef]

173. Tobisch, S. Copper hydride-mediated electrophilic amidationof vinylarenes with dioxazolones–a computationalmechanistic study. *Dalton Trans.* **2019**, *48*, 14337–14346. [CrossRef]

174. Yuan, Y.; Wu, F.-P.; Schünemann, C.; Holz, J.; Kamer, P.C.J.; Wu, X.-F. Copper-Catalyzed Carbonylative Hydroamidation of Styrenes to Branched Amides. *Angew. Chem. Int. Ed.* **2020**, *59*, 22441–22445, For a related Cu-H catalyzed hydroamidation process using CO. [CrossRef]

175. Ye, Y.; Kim, S.-T.; Jeong, J.; Baik, M.-H.; Buchwald, S.L. CuH-Catalyzed Enantioselective Alkylation of Indole Derivatives with Ligand-Controlled Regiodivergence. *J. Am. Chem. Soc.* **2019**, *141*, 3901–3909. [CrossRef]

176. Ye, Y.; Kevlishvili, I.; Feng, S.; Liu, P.; Buchwald, S.L. Highly Enantioselective Synthesis of Indazoles with a C3-Quaternary Chiral Center Using CuH Catalysis. *J. Am. Chem. Soc.* **2020**, *142*, 10550–10556. [CrossRef]

177. Zhu, S.; Niljianskul, N.; Buchwald, S.L. A Direct Approach to Amines with Remote Stereocentres by Enantioselective CuH-catalysed Reductive Relay Hydroamination. *Nat. Chem.* **2016**, *8*, 144–150. [CrossRef]

178. Shi, S.-L.; Wong, Z.L.; Buchwald, S.L. Copper-catalysed Enantioselective Stereodivergent Synthesis of Amino Alcohols. *Nature* **2016**, *532*, 353–356. [CrossRef]

179. Guo, S.; Zhu, J.; Buchwald, S.L. Enantioselective Synthesis of β-Amino Acid Derivatives Enabled by Ligand-Controlled Reversal of Hydrocupration Regiochemistry. *Angew. Chem. Int. Ed.* **2020**, *59*, 20841–20845. [CrossRef]

180. Shi, S.-L.; Buchwald, S.L. Copper-catalysed Selective Hydroamination Reactions of Alkynes. *Nat. Chem.* **2015**, *7*, 38–44. [CrossRef]

181. Nishino, S.; Hirano, K.; Miura, M. Cu-Catalyzed Reductive gem-Difunctionalization of Terminal Alkynes via Hydrosilylation/Hydroamination Cascade: Concise Synthesis of α-Aminosilanes. *Chem. Eur. J.* **2020**, *26*, 8725–8728. [CrossRef]

182. Arbour, J.L.; Rzepa, H.S.; White, A.J.P.; Hii, K.K.M. Unusual Regiodivergence in Metal-catalysed Intramolecular Cyclisation of γ-Allenols. *Chem. Commun.* **2009**, 7125–7127. [CrossRef]

183. Chou, T.-H.; Yu, B.H.; Chein, R.-J. ZnI$_2$/Zn(OTf)$_2$-TsOH: A Versatile Combined-acid System for Catalytic Intramolecular Hydrofunctionalization and Polyene Cyclization. *Chem. Commun.* **2019**, *55*, 13522–13525. [CrossRef]

184. Ghobadi, M.; Qhazvini, P.P.; Kazemi, M. Catalytic application of zinc (II) bromide (ZnBr$_2$) in organic synthesis. *Synth. Commun.* **2020**, *50*, 3717–3738. [CrossRef]

185. Li, T.; Wiecko, J.; Roesky, P.W. Zinc-catalyzed hydroamination reactions. In *Zinc Catalysis: Applications in Organic Synthesis*; Enthaler, S., Wu, X.-F., Eds.; Wiley-VCH Verlag GmbH & Co. KGaA: Weinheim, Germany, 2015; pp. 83–118.

186. Zulys, A.; Dochnahl, M.; Hollmann, D.; Löhnwitz, K.; Herrmann, J.S.; Roesky, P.W.; Blechert, S. Intramolecular hydroamination of functionalized alkenes and alkynes with a homogenous zinc catalyst. *Angew. Chem. Int. Ed.* **2005**, *44*, 7794–7798. [CrossRef]

187. Duncan, C.; Biradar, A.V.; Asefa, T. Aminotroponate/aminotroponiminate zinc complexes functionalized mesoporous silica catalysts for intramolecular hydroamination of non-activated alkenes with varied steric and electronic properties. *ACS Catal.* **2011**, *1*, 736–750, For an interesting supported version of aminotroponiminate-/aminotroponate-zinc complexes. [CrossRef]

188. Chilleck, M.A.; Hartenstein, L.; Braun, T.; Roesky, P.W.; Braun, B. Cationic zinc organyls as precatalysts for hydroamination reactions. *Chem. Eur. J.* **2015**, *21*, 2594–2602, For a triple-decker complex [Zn2Cp*3]+ [BArF4]- that demonstrates high catalytic activity in hydroamination without a co-catalyst. [CrossRef] [PubMed]

189. Mukherjee, A.; Sen, T.K.; Ghorai, P.K.; Samuel, P.P.; Schulzke, C.; Mandal, S.K. Phenalenyl-based organozinc catalysts for intramolecular hydroamination reactions: A combined catalytic, kinetic, and mechanistic investigation of the catalytic cycle. *Chem. Eur. J.* **2012**, *18*, 10530–10545. [CrossRef]

190. Mukherjee, A.; Sen, T.K.; Ghorai, P.K.; Mandal, S.K. Organozinc catalyst on a phenalenyl scaffold for intramolecular hydroamination of aminoalkenes. *Organometallics* **2013**, *32*, 7213–7224. [CrossRef]

191. Shen, X.-J.; Bu, H.-Z.; Shi, J.; Wu, Z.-G.; Ma, H.-F.; Li, Y.-F. Zn(CF$_3$SO$_3$)$_2$-mediated domino hydroamination-ring cleavage of 2,5-dihydrofuran. *Tetrahedron Lett.* **2013**, *54*, 3937–3939. [CrossRef]

192. Barman, M.K.; Baishya, A.; Nembenna, S. Bulky guanidinate calcium and zinc complexes as catalysts for the intramolecular hydroamination. *J. Organomet. Chem.* **2019**, *887*, 40–47. [CrossRef]

193. Horrillo-Martinez, P.; Hultzsch, K.C. Intramolecular hydroamination/cyclization of aminoalkenes catalysed by diamidobinaphthyl magnesium- and zinc-complexes. *Tetrahedron Lett.* **2009**, *50*, 2054–2056. [CrossRef]

194. Hussein, L.; Purkait, N.; Biyikal, M.; Tausch, E.; Roesky, P.W.; Blechert, S. Highly enantioselective hydroamination to six-membered rings by heterobimetallic catalysts. *Chem. Commun.* **2014**, *50*, 3862–3864, For a highly enantioselective cyclization of aminohex-1-ene type substrates by a Zr-based catalyst stabilized by a zinc-salen metalloligand. [CrossRef]